Autonomously Deployable Tower Infrastructure for Exploration and Communication in Lunar Permanently Shadowed Regions

Caleb Amy[1], Marc-André Bégin[1], Becca Browder[2], Manwei Chan[3], Charles Dawson[4], Paula do Vale Pereira[3], Travis J. Hank[4], Eric Hinterman[3], George Lordos[5], Benjamin Martell[4], Alex Miller[6], Cormac O'Neill[7], Vineet J. Padia[8], Natasha Stamler[9], Jessica Todd[10], Nieky Wang[11], Dava J. Newman[12], Olivier L. de Weck[13], Jeffrey A. Hoffman[14]

Massachusetts Institute of Technology, Cambridge, MA 02139, USA

Massachusetts Space Grant

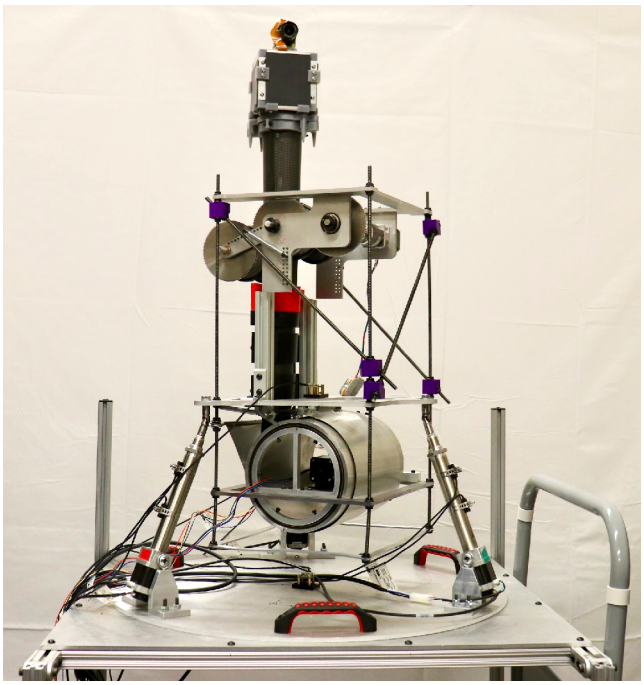

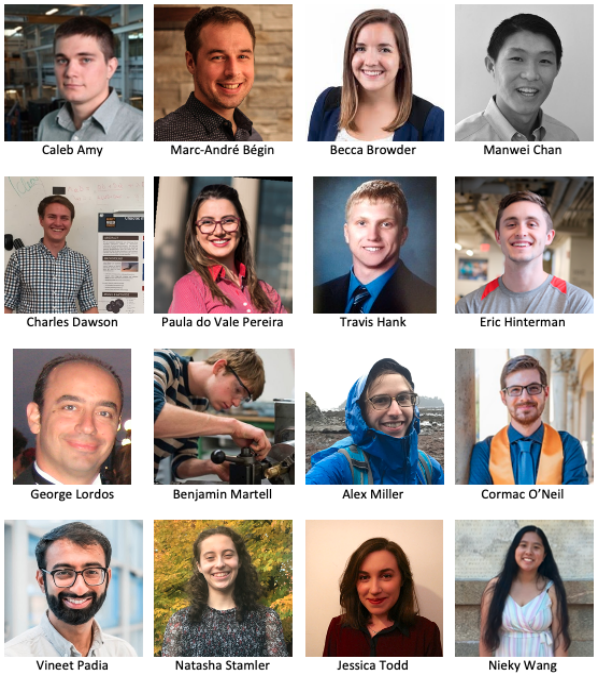

[1] PhD Candidate, Dept of Mechanical Engineering
[2] MS Candidate, Dept of Aeronautics and Astronautics and Technology & Policy Program
[3] PhD Candidate, Dept of Aeronautics and Astronautics
[4] MS Candidate, Dept of Aeronautics and Astronautics
[5] (Team Lead) PhD Candidate, Dept of Aeronautics and Astronautics
[6] Undergraduate Student, Physics and EECS
[7] MS Candidate, Dept of Mechanical Engineering
[8] Research Scientist, Dept of Mechanical Engineering
[9] Undergraduate Student, Mechanical Engineering and Urban Planning
[10] PhD Candidate, Dept of Aeronautics and Astronautics and Woods Hole Oceanographic Institute
[11] Undergraduate Student, Mechanical Engineering
[12] Apollo Professor of Aeronautics and Astronautics, Dept of Aeronautics and Astronautics
[13] Professor of Aeronautics and Astronautics and Engineering Systems, Dept of Aeronautics and Astronautics
[14] Professor of the Practice of Aeronautics and Astronautics, Dept of Aeronautics and Astronautics

MIT – Multifunctional Expandable Lunar Lightweight Tall Tower (MELLTT)

Concept Synopsis

MELLTT creates a line-of-sight from a CLPS lunar lander to other areas of the lunar surface and into the interior of a PSR. This allows for communication, power beaming, and imaging to support distal assets, as well as stand-alone remote sensing of PSR interiors. This Earth proof-of-concept autonomously levels to accommodate landing on a slope, deploys a 2m composite boom, and elevates a standard 1U payload to provide the line-of-sight.

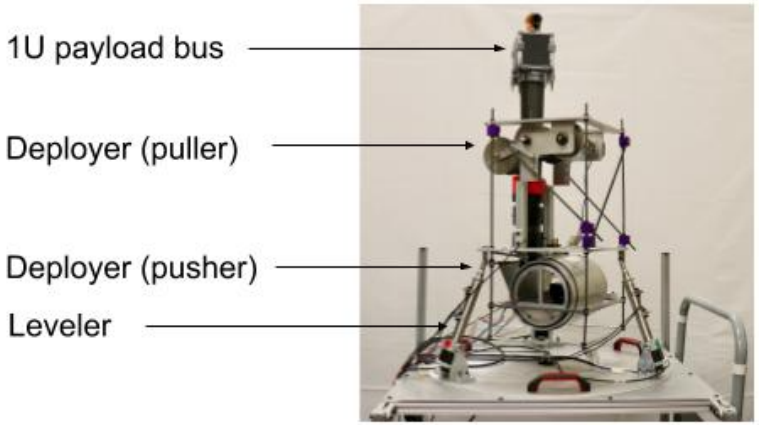

Innovations

- Proved that composite, deployable booms can be deployed against a gravity vector, while previous demonstrations have only been done in microgravity.
- Demonstrated a lightweight and compact way to elevate equipment on the lunar surface using COTS components and existing lander designs.
- Developed a standardized (derived from U-class spacecraft) payload bus to allow for ready adaptation of MELLTT to a variety of client payloads.

Proof-of-Concept Testing Results & Conclusions

- An Earth-based prototype has successfully demonstrated boom deployment and retraction, self-leveling up to 12° while bearing a 34 kg load, and re-orienting of the payload bus to allow for remote sensing.
- The deployed boom's response to external disturbances is characterized and shown to be stable against toppling within expected lunar conditions.
- The MELLTT concept is now at TRL 4 and longer booms (6m, 16.5m) will be tested in AY 2020-2021 following delays due to COVID.

I. EXECUTIVE SUMMARY

The environment inside lunar polar permanently shadowed regions (PSRs) is challenging for robotic and human explorers with extreme cold, vacuum, extended darkness, ice as hard as basalt, difficult terrain, and the limited or non-existent line of sight to the lunar surface. With these difficulties in mind, this MIT project primarily addresses the BIG Idea Challenge area of "capabilities to explore and operate in PSRs." Taking advantage of the relatively weak lunar gravitational field, the team's concept of a tall, lightweight, autonomously deployed tower with a payload deck on top, situated just outside the PSR, will validate a viable design for a lunar tower capable of supporting an extended ecosystem within or around PSRs, alleviating limitations imposed by the terrain of those regions. The tower would provide multiple lines of sight to the Earth, the Sun, the lander, the interior of the PSR and the lunar surface, so that payloads at the top of the tower could image the area and provide communications and power beaming to small, distributed assets that operate in and around PSRs.

The utility of deployable towers on the lunar surface, including various payload applications, was studied by another group of MIT students who envisioned a lunar PSR exploration ecosystem supported and enabled by MELLTT [1].

This paper describes the design and development of MELLTT from TRL 1 to 4. The MELLTT project began in October 2019 and will culminate in a TRL 4 demonstration at the NASA BIG Idea Virtual Forum in January 2021. As part of the project, a preliminary design review (PDR) and a critical design review (CDR) were conducted with MIT, NASA and industry advisers. The reviews demonstrated that the MELLTT design closed for a deployable tower that can elevate a 5kg payload to a demonstration height of up to 16.5 m above a lunar lander deck. Due to COVID-19, a planned loan of a 16.5 m composite boom from NASA Langley Deployable Composite Booms (DCB) team did not proceed. For the purposes of the first prototype, NASA lent a 2 m composite boom to the team, and a commercial 6 m composite boom of a different design has been procured and will be integrated with the hardware.

As of the time of writing of this paper, the majority of subsystem and system assembly, integration and testing is complete, with only a few minor refinements remaining before the final demonstration. Starting from a tilted mock lander deck, MELLTT will self-level, gradually deploy the boom to full height, and demonstrate nominal operations of the elevated platform. The demonstration payload will consist of a solar-powered radio repeater and a RGB camera integrated within a 1U CubeSat capable of rotating to a desired azimuth, showing how the operational capabilities of other robotic assets within and near the PSRs can be enhanced and supported by MELLTT.

The design, development, testing and planned demonstration described in this paper comprise the first phase of a complete path-to-flight strategy for the MELLTT architecture. The development plan includes component, functional, and simulated surface operations testing to verify the proposed system design, aiming for readiness to support near-term lunar technology demonstration missions with as-yet unfunded flight designs that have been proposed to NASA. The MIT team is pursuing additional funding for deployable lunar towers with NASA and industry collaborators.

II. PROBLEM STATEMENT AND BACKGROUND

In the lead-up to the planned Artemis crewed landings, a fundamental, short-term need for NASA and its international and commercial partners will be to robotically explore and understand the challenging environments in and around PSRs. Previous remote sensing missions have detected the presence of volatile deposits, including water, that have the potential to enable in-situ resource utilization (ISRU) in these regions. Gaining a deeper understanding of the distribution and quantity of resources in PSRs is critical for sustained exploration of the lunar surface. However, the environment within PSRs presents significant operational challenges for autonomous and crewed systems. Temperatures average below 50K, and the low visibility and challenging terrain make traversing highly risky. Lack of sunlight and poor lines-of-sight out of PSRs pose significant challenges for power generation and communication.

A key goal of the Artemis program is the development of a sustainable foundation for medium and long-term lunar settlement. A second capability that would be highly beneficial for any long-term lunar operation is the development of distributed regional networks to support high-bandwidth data, communication, situational awareness, and navigation. Such a network could be utilized by space agencies and private companies to support remote assets on the surface, or human explorers.

To address the short-term need for exploring PSRs, and with the desire to build technical capability towards a longer-term goal of establishing lunar regional networks, MIT presents the Multifunctional Expandable Lunar Lightweight Tall Tower (MELLTT). MELLTT is a lightweight, self-deploying tower capable of deploying from a lunar lander near the rim of a crater containing a PSR. A tower located near the edge of a PSR could enable line-of-sight communication and power transmission to assets within the PSR and support short- and medium-range remote sensing into these regions with resolutions much finer than those provided by orbital systems. The goal of the MELLTT project is to chart a path-to-flight for an initial prototype of a deployable tower capable of providing supporting services (situational awareness and data) to small robotic assets in and around a PSR, raising the technology readiness level (TRL) of low-cost lightweight tower systems that could be utilized for long-term operations.

III. PROJECT DESCRIPTION

III.I Overview

The MELLTT system is a technology demonstration of a lightweight, self-deploying and self-leveling tower for exploration of PSRs on the lunar surface (Fig. 1). The MELLTT prototype is designed around a space-proven, lightweight carbon-fiber composite boom that is rolled flat on a spool and takes the shape of a rigid cylindrical mast upon unspooling [2,3]. A leveler subsystem aligns the deployer subsystem with the lunar gravity field, and a self-powered elevated payload platform at the top of the composite boom hosts imaging and communications demonstration payloads. A sensor system comprised of three accelerometers mounted on each subsystem, as well as a photogrammetry experiment (which is not yet complete, but is targeted for completion by the final demonstration date) mounted on the leveler base, collect engineering data used during deployment and operations, which will inform the design of future generations of lunar towers. A detailed description of the various subsystems is given in Section III.VII.

A set of system functional requirements was developed based on the problem statement above (Section II), as shown in Table 1.

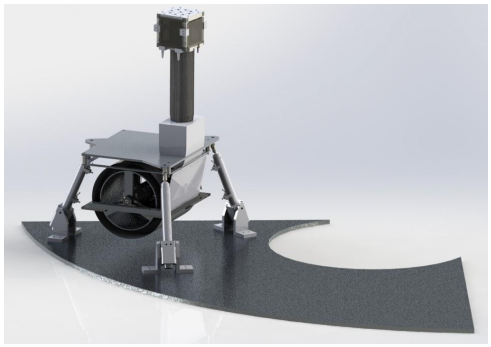

Figure 1: A rendering of the MELLTT tower showing the lander deck, leveling subsystem, deployer subsystem, the partly-deployed composite boom and the elevated demonstration payload.

Table 1: System Functional Requirements

ID	System Functional Requirement	Justification
S01	The system must provide lines-of-sight between third-party payloads on the upper	This is the main functional deliverable of the system. Multiple lines of sight meet at the top of

	platform and the interior of the PSR, the surroundings and/or other deployed assets as needed.	the tower and support remote science and exploration by an ecosystem of small, deployed robotic equipment.
S02	The system must provide third-party payloads fixed to the upper platform with launch mount, power, data, pointing, sun sensing, leveling and situational awareness.	The upper platform provides standardized services to payloads with a view to reducing payload size, cost and development time.
S03	The system must adhere to constraints of the NASA CLPS lunar lander design.	Requirement of the 2020 NASA BIG Idea Challenge
S04	The demonstration system shall utilize flight proven equipment wherever possible.	To shorten the path to flight and meet the 2023 launch goal.
S05	The system shall return engineering data suitable for the validation of the current design and for designing the next generation of towers.	Data from the landing, deployment and operations phases of the first prototype tower will inform the design of taller, larger towers that can support more advanced payloads.

III.II Technology Demonstration Goals

MELLTT has successfully accomplished its two primary technical goals: (1) demonstration of the autonomous leveling and construction of a fixed lightweight tower, and (2) development of a standard payload platform atop the tower capable of supporting various types of payloads for exploration and operation in PSRs. These technology goals raised the TRL of deployable towers to enable future lunar infrastructure and take advantage of the elevated platform to support a range of payloads.

Lunar Infrastructure Development

By deploying multiple MELLTTs near a PSR exploration zone, future missions to the same region can enjoy increased operational capabilities at reduced costs. MELLTT infrastructure supports the improved range and reliability of regional surface communications, stereoscopic mapping and real-time situational awareness in the vicinity of landers, identification of potential routes into or out of a PSR, and wireless energy transfer in the form of reflected sunlight, microwaves or lasers. [1] With future lunar infrastructure functionality in mind, MELLTT is being designed from the outset with a goal of outliving its host lander. The leveler's locking mechanism is passive, requiring no power from the lander to hold its leveled pose. In addition, the oblique angle of incidence of sunlight at the lunar pole makes some high-elevation regions experience near-constant illumination, so that solar panels at the top of the tower will be more consistently illuminated than panels on the lander. This could allow the elevated payload platform to capture energy with which to continue providing services to nearby assets, turning older towers into longer-lived infrastructure that forms part of an expanding regional network.

Elevated Payload Platform

Anticipating the need to cater to many applications, lower costs and raise the TRL at component level for faster deployment by building on heritage space hardware, the elevated payload platform in the MELLTT concept is a CubeSat, offering "plug and play" services of standard mounting, power solutions and data interfaces to a range of hosted payloads that can benefit from the multiple lines of sight. The avionics and communications system provide plug-and play data, control, and telemetry services to the elevated payloads. In addition, MELLTT's elevated platform and its client payloads will be independently powered by fixed solar cells on all four vertical sides of the CubeSat, providing simplicity and security of power supply to the payloads. This power source also supplies an actuator to rotate the platform,

delivering an azimuthal pointing capability, useful to payloads such as imagers and high gain antennas. The MELLTT prototype features a 1U CubeSat.

III.III Science Goals

The primary science goal of the MELLTT system is to provide capabilities to explore and operate in PSRs. MELLTT's elevated payload platform is key to enabling NASA's science goals of exploring PSRs for volatiles such as water. The elevated payload deck provides a line-of-sight into PSRs for imaging systems such as high resolution cameras or multispectral images, providing order-of-magnitude higher-resolution data than is obtainable from orbital assets. Such systems would be capable of characterising obstacles and improving spatial resolution maps of PSRs, thus improving navigation for any robotic assets in the region. Infrared visible light payloads could be utilized to capture evidence of volatiles and water, as well as characterise the geomorphology and chemical composition of lunar regolith within the PSR. An elevated payload deck also provides the opportunity for wireless power beaming to assets within the PSR, such as the 50 W, 5km range laser system proposed in [1]. Such a system would enable small rovers to perform long-term exploration missions within PSRs without relying on solar- or RTG-based power systems. A more detailed explanation of potential scientific and operational applications of MELLTT is explored in the companion paper [1].

III.IV Key Stakeholders

The initial key stakeholders for MELLTT will be NASA and other space agencies interested in scientific exploration of the lunar surface. The work presented in this report marks the first phase of the project, focused on initial proof-of-concept and technology demonstration. An initial flight demonstration could carry a small scientific payload to image PSRs, which would lay the groundwork for further robotic and eventual human exploration of PSRs.

As stated above, the successful proof-of-concept and increased TRL resulting from this study makes such lightweight towers appealing to a variety of commercial entities. The plug-and-play payload deck could easily support payloads from small commercial entities interested in data gathering about PSRs, potentially for applications of resource utilization. A scaled up system capable of supporting heavier payloads, or a distributed network of lightweight MELLTT towers (as is explored in [1]), would have wide ranging applications for commercial stakeholders to begin large scale operations on the lunar surface. Several commercial companies have already expressed interest in the MELLTT system, as evidenced by their collaboration with the MELLTT team in submitting a proposal to NASA's LuSTR solicitation.

III.V Key Assumptions and Constraints

MELLTT's key assumptions and constraints were driven by the lunar landing system. MELLTT was assumed to be deployed off a NASA CLPS lander. [4] It is assumed the lander has the capability to land within 100m of a PSR crater wall. This drove the sizing of the tower height. The Astrobotic design and Payload User Guide (PUG) [5] was assumed to be the CLPS lander, as this system has the most complete data available. The main CLPS constraints applicable to the MELLTT design were:

Table 2: NASA CLPS lander constraints

Category	Constraint
Mass	● Limit of 15kg
Power	● At least 8 W continuous and 40 W peak for 5 minutes ● Regulated and switched 28 VDC
Communications	● Bandwidth (rate at which data can be sent to the lander): At least 70 kbps per kg of payload (if more is needed, internally store/buffer to stay under 70 kbps)

	• RF comm (rate at which comm can be relayed to Earth): 70 kbps per kg max (if more is needed, internally store/buffer to stay under 70 kbps) • Wireless comm: 2.4 GHz IEEE 802.11n compliant WiFi
Mounting	• MELLTT was designed to be mounted on the top deck of the Astrobotic Peregrine lander. The top deck was approximated as a 1m² square platform.

In addition to these constraints, the team added another constraint based on CLPS capabilities: the ability to level the system. While CLPS providers appear to be designing leveling systems into their landers in order to accommodate landing on a slope on the lunar surface, being level is critical for MELLTT's tower deployment, so a leveler was included in the system design. Based on a literature review, the team determined that the system should be able to level up to 12° to accommodate a wide range of landing locations on the Moon. While some CLPS landers may perform their own leveling, the lander capabilities are still in development, so it was critical for MELLTT to be able to self-level in the event of landing on a slope that exceeds a CLPS lander's leveling limit.

III.VI Concept of Operations

Fig. 2 shows the flight concept of operations for MELLTT for a lunar-rated system. Following delivery to the lunar surface by a Commercial Lunar Payload Services (CLPS) landing system, MELLTT will be deployed directly from the landing platform. The *Deployment* phase of operations will last approximately 1 Earth day. Initial leveling will take place to account for lander incline prior to deployment. The tower is then deployed and if leveling sensors detect a severe deviation equivalent to a lateral warp beyond approximately 1% of boom length the deployer is halted while the system self-levels. Following full deployment and a full checkout of all subsystems, the *Operations* phase begins, providing a full lunar polar day (13 Earth days) for payload operations. The first lunar demonstration of MELLTT will include camera tests (rotations and stereo image depth sensing), pointing test to test the accuracy of the rotational payload platform and the stability of the tower, and testing of the independent payload deck power system.

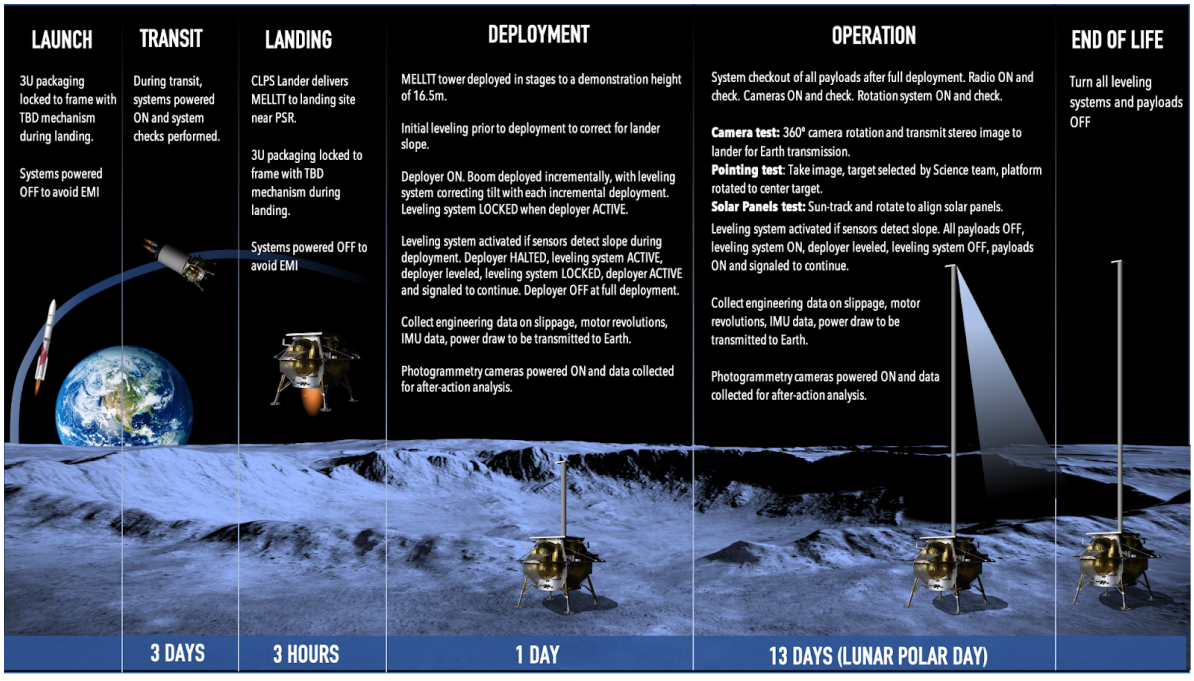

Figure 2: Concept of operations for MELLTT on the lunar surface

For the Earth proof-of-concept demonstration of MELLTT, only the deployment and operation phases were considered. A mock lunar lander (discussed below) was constructed to emulate the power supply, mounting and possible landing inclination of a true CLPS lander.

III.VII Subsystem Designs

Leveling Subsystem

The tower deployer is mounted onto a dynamic base capable of leveling the tower with the use of a sensing and actuator system. Given the full height of the lunar tower at 16.5 m, a small deviation in incline at the base would create a large moment arm and risk tipping or warping the tower. This self-leveling base has three primary functions: (1) align the tower with the lunar gravitational field to account for any incline in the terrain of the landing site, (2) compensate for any shift in lander or tower position caused by deployment of other payloads, moonquakes [6,7] or other vibrations or shocks, and (3) allow the angle of the deployed tower base to be adjusted to account for boom bending. The leveling system design is a modified Stewart platform [8] consisting of a deployer mounting plate supported by three linear actuators attached with universal joints. These actuators are mounted directly onto the lander platform with trunnion mounts, providing hinge action. The actuators can adjust the platform in two rotational degrees of freedom (roll and pitch) and one translational degree of freedom (height) to achieve leveling of up to ± 12° off the horizontal plane. Based on current documentation, commercial lunar landers will not attempt to land on slopes greater than 12° [5]. The deployer is mounted into the deployer plate as shown in Fig. 3. The linear actuator legs are controlled using stepper motors.

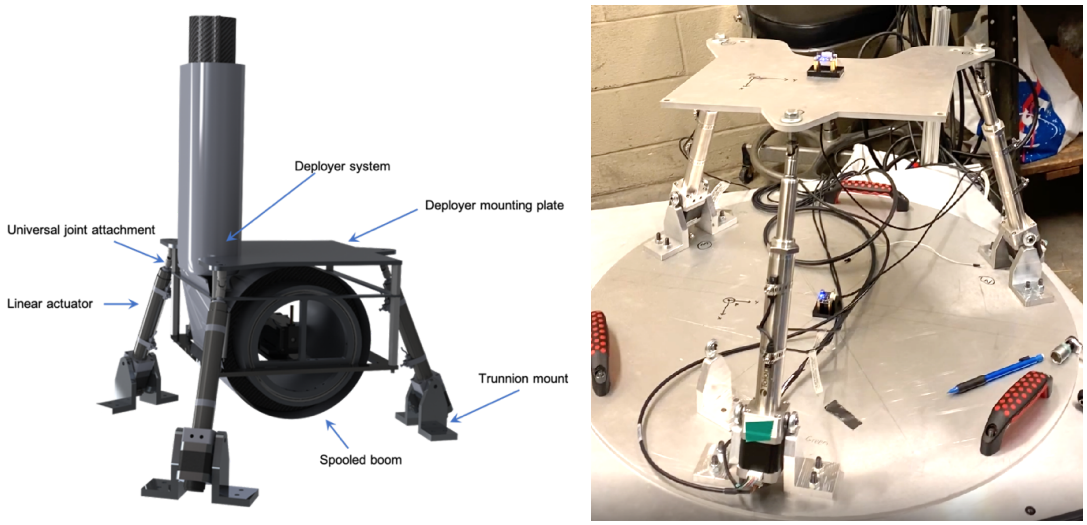

Figure 3: (Left) CAD rendering of the self-leveling tower base and (right) Leveler prototype being tested in the lab.

The system uses Tinkerforge accelerometer units, consisting of three-axis accelerometers integrated into a single chip, mounted onto the deployer plate, lander platform and payload platform, to determine the orientation of the tower relative to the gravity gradient. Forward kinematics use this sensor data to determine the current pose and attitude of the leveling platform. Inverse kinematics are used in real time to determine the required linear actuator extensions for the desired platform pose and attitude and an open-loop controller used for initial leveling. The desired pose and attitude is fine-tuned using closed-loop feedback control based on accelerometer data. The feedback controller will continue to level until the norm of the deployer plate is within 1% of the gravity vector. Further details of the forward and inverse kinematics can be found in Appendix A.

When powered off, the leveling system remains locked in position. To avoid resonance or unwanted vibrations in the tower, the leveling system does not continually level the system during deployment and

operation. The tower base is designed to actively self-level at fixed intervals during the deployment phase, as discussed in the concept of operations, as well as enabling manual leveling via operator input. The accelerometers remain active during operation to detect any change in inclination or boom bending, at which point the leveling system can be switched on to actively level if an incline is detected. Both the manual and automatic leveling of the system have been successfully tested and proven to work as expected.

Deployment Mechanism Subsystem

The deployer design is shown in Fig. 4a (i) and is based on an aluminum spool which is powered by a stepper motor to push the boom through a bracing system, which supports it during transition from a flat to a deployed cross-sectional shape. After the transition brace, the boom is pulled by a powered system of rollers, depicted in Fig. 4a (iii), which is situated at the top of the bracing mechanism. These rollers grip the flat edges of the double-omega boom, helping to hold the weaker section of the boom beneath it in tension; the rollers are designed to automatically and dynamically grip around the boom with a uniform grasping pressure and low spring tension, similar to the uniform pressure in a cylindrical pressure vessel without causing cracking or crumpling. Several different roller geometries were designed, so that an iterative testing process could be used to evaluate different configurations. The motor and corresponding 256x1 gearbox were sized to provide approximately 5x the estimated torque required to overcome Earth's gravity and friction to allow for terrestrial testing and sufficient safety factor.

The deployer includes two types of bracing. As the boom is unspooled, blossoming is prevented by a low friction surface held tightly around the boom by springs. To prevent buckling due to the gravitational loads during the boom's transition from flat to lenticular, a fully-enclosed 3D-printed structure shown in Fig. 4b (ii) lends significant support, with an additional goal of low friction operation.

The deployer is designed to deploy both types of booms, with only a different shaped 3D printed brace needed for the different cross sectional shapes.

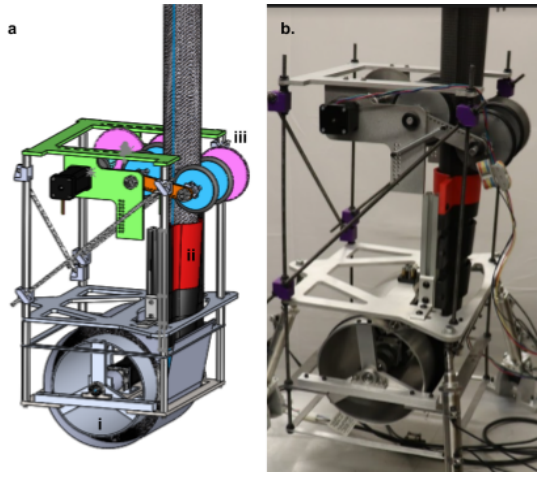

Figure 4: a. The CAD design of the deployer integrated with the lenticular boom. b. The Earth prototype of the deployer integrated with the boom and the leveler. i) The boom is wrapped around a 6" spool that pushes the boom through the ii) 3-D printed brace, which guides the boom from flat to deployed. iii) The roller system pulls the boom out, overcoming any blooming or excess friction caused by the bracing systems. Reversing the direction of i) and iii) allows retraction.

Tower Subsystem

The tower structure is based on a flight-heritage deployable composite boom concept that has been used in microgravity situations on board satellites. These booms are typically stored rolled up flat in a spool during space travel. Once the desired location is reached, the spool unravels, deploying a straight boom that naturally takes its shape. These composite booms can take many different cross sectional shapes, the most common being the C-shaped boom, seen in Fig. 5b. MELLTT is testing both a C-shaped boom with

a slit-lock technology, as well as a lenticular shaped (double-omega) boom, seen in Fig. 5a. The lenticular boom was loaned to the MELLTT team by NASA Game Changing Development's (GCD) Deployable Composite Boom (DCB) Research group. It is 2 meters long, has a total flattened length of 130 mm, and when deployed has a diameter around 75 mm. The thickness of this boom varies depending on the section of the boom, from 0.183 to 0.241 mm. The majority of testing has thus far employed this lenticular boom; however, the MELLTT team has also purchased a differently shaped boom for future testing to compare performance in gravity fields and under torsional disturbance conditions. The other boom is a similar diameter, 76.2 mm, but has a C-shaped cross section and uses Slit-Lock to reduce torsional instability. Both a 2 m and a 6 m boom were purchased from Composite Technologies Development (CTD), one of which is shown in Fig. 5b. This boom is a uniform 0.381 mm thickness.

Neither of these types of booms have been tested in lunar gravity before. The main objective of this study is to determine the feasibility, challenges, and benefits of using deployable composite boom in lunar gravity to support a payload at the top, as well as to develop the supporting infrastructure mechanisms to ensure a safe, vertical, and reliable deployment.

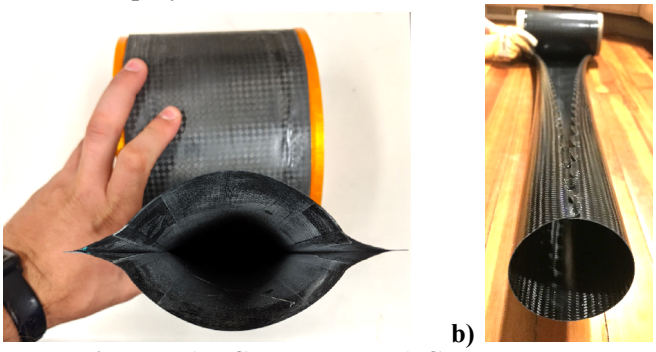

a) **b)**

Figure 5 a) DCB boom and b) CTD boom

Elevated Payload Platform Subsystem

To provide client payloads with access to the benefits of an elevated vantage point, the MELLTT system includes a payload platform mounted to the top of the tower. This platform is modelled on a 1U CubeSat with exterior solar panels on the four sides and a top deck with patterned mounting holes (Fig. 6a), with most of the interior volume taken up by a motor for pointing, battery and avionics packaged, as shown in Fig. 6b. The primary function of the elevated payload platform is to provide a standardized interface for mounting client payloads, while providing power and communications services, and azimuthal pointing for payloads. Our use of the CubeSat form factor allows us to leverage readily available space-heritage CubeSat hardware, shortening the path to flight while increasing its reliability and standardization. The design of the interface with client systems is discussed in Section III.X (Integration with External Systems).

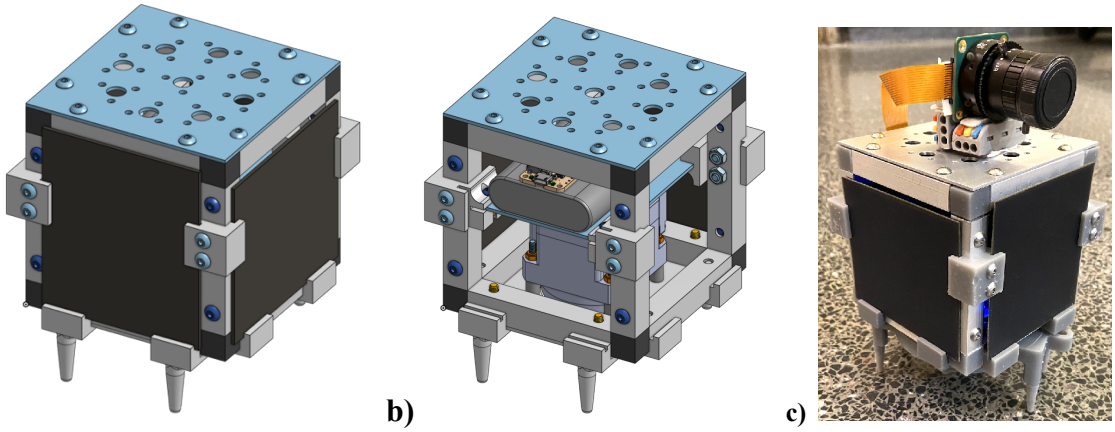

a) **b)** **c)**

Figure 6 a) The 1U payload platform, with standardized mounting for client payloads on the upper surface of the platform. b) Interior view showing pointer motor (larger block near the bottom of the CubeSat), battery (large block above the motor) and avionics. Client payloads are mounted on the top deck. c) Integrated payload platform carrying a RGB camera.

The azimuthal pointing capability is provided by an internal servo motor, which rotates the entire payload platform about the long axis of the boom, allowing not only for precise pointing of client payloads but also for redundant power generation, since solar tracking can be employed to compensate for the loss of up to two solar panels. As a demonstration of a potential client, a camera was mounted to the top of the payload platform. This camera stands in for scientific instruments that would seek to leverage the increased line of sight provided by MELLTT for remote studies of the lunar surface and PSRs. Images from this camera will demonstrate the line of sight improvements provided by the tower and will be streamed to the lander.

The platform also includes self-contained power and communications subsystems to provide services to the client payloads. The communications subsystem contains a short-range WiFi link for communicating between the payload platform and lander.

The power generation (solar cells) and storage (batteries) subsystem is completely isolated from the lander and tower-base power systems. This subsystem powers the radio, client payloads and the pointing motor. The isolation of the payload power subsystem means that the payload platform is capable of surviving the death of the lander during the lunar night at the poles, since the elevated platform will have access to solar power for an extended time due to the high angle of solar incidence at the lunar poles. The power subsystem includes a lithium polymer battery with 22.2 Wh storage capacity, four solar panels mounted around the outside of the platform with 2.7 W combined generation capacity, and charging and distribution components producing regulated 5 V and 12 V power buses. The team considered two modes of primary operation: a nominal mode and a low power mode. Nominal operation leads to a power draw of 0.03W, while the low power mode charges the battery at a rate of 1.14 W (Table B-1). For the purposes of a terrestrial demonstration, the system is designed to operate for 6 hours: an initial 4 hours of nominal use, followed by 0.5 hours of low-power operation, before a final 1.5 hours of nominal use.

The payload platform connects to the deployable composite boom via a custom-designed interface, which was 3D printed for this prototype. This interface connects at one end to the internal servo motor on the payload platform (with a thrust bearing to isolate the motor from axial loads), and it connects at the other end to the boom via clamps designed to match the profile of the composite boom when fully deployed. The interface also includes pegs (visible in Fig. 6) that register with holes in the upper surface of the deployer, locking the payload platform into place and constraining its movement in the x and y directions during transportation and cruise phases.

During the design of the payload subsystem, a conservative mass estimate of 2.27 kg with a 20% margin was used. However, this turned out to be a significant overestimate as the final prototype system ended up with a mass of 1.2 kg (Table B-2).

Command and Control Subsystem

The control system is constructed in the Robot Operating System (ROS) framework that provides a simple method to interface subsystems through standard messaging for sensors and actuators. Fig. 7 summarizes the logical components along with their physical or software interfaces.

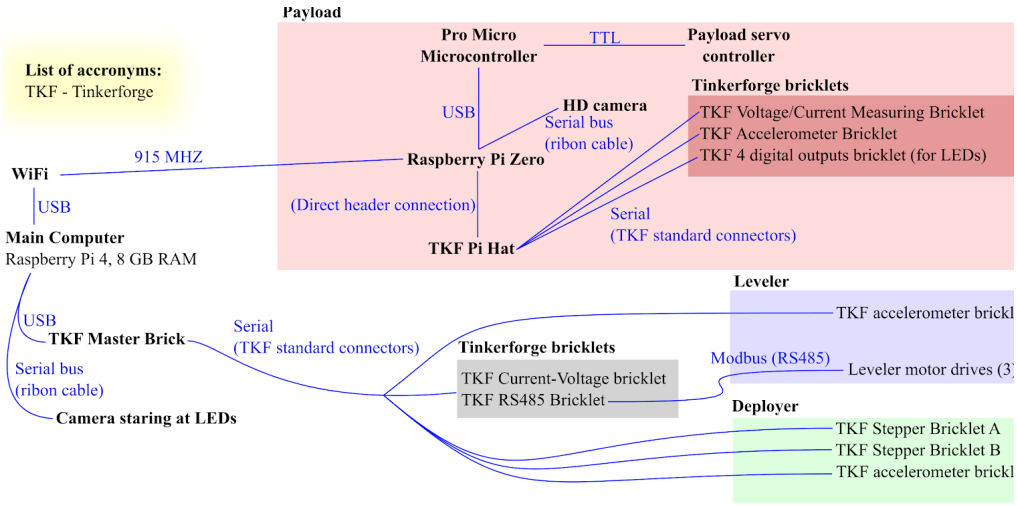

Figure 7: System diagram of logical components and their interfaces.

Onboard the elevated platform subsystem, a Pi Zero computing module captures images from a camera and controls the rotation of the platform, thereby enabling high resolution panoramic footage. The power consumption and acceleration of the elevated platform are also measured. Measuring the power consumption allows us to test the performance of the system within the intended power budget, and the acceleration measurement provides both redundancy for computing the gravity vector for leveling and facilitates characterization of boom movement and vibrations. The images and acceleration data received from the payload are transmitted via a short-range WiFi link to the lander.

To better assess the static deflections of the elevated platform, a monocular photogrammetric method is being implemented to estimate the platform pose [9], consisting of a high definition camera on the lander with an IR-Pass filter to image four infrared LEDs that shall be installed on the bottom surface of the platform. Four LEDs were chosen because the full pose of the platform can be reconstructed by tracking the distances between the LEDs. The IR-Pass filter in combination with IR LEDs is an effective method to increase the contrast of the images and filter out background noise.

In both the lander and elevated platform, power diagnostics are important to prevent damage by monitoring power from the solar panels and power supply. The MELLTT system has the ability to actively sense both the current and voltage, and minimize failure by shutting down problematic components.

Within the deploying subsystem, Tinkerforge stepper motor controllers are used to implement closed-loop control of the motor position and velocity.

The leveling subsystem uses multiple layers of controllers to achieve its purpose of leveling the tower. At a low level, third-party motor controllers (Tolomatic ACS stepper driver) are used to implement closed-loop control of the three linear actuator stepper motors. Three cascaded control loops on velocity, position and torque allow each leg to extend to its commanded length within predefined speed and force limits. A single Tinkerforge RS485 Bricklet is used as a Master device to communicate with the three motor controllers using the daisy-chain property of Modbus RTU communication protocol. At a high level, the main computer, a Raspberry Pi 4B, computes the current and desired pose of the leveling system as well as the corresponding leveler leg lengths. From the known kinematics of the leveling platform and given the orientation of the gravity vectors measured by the Tinkerforge accelerometers placed on the system, the main computer first determines what the length of each leg should be using inverse kinematics (see Appendix A). Once each leg achieves its desired position, the computer then uses closed-loop compensation on the pitch and roll of the platform until the tilt of the platform with respect to the gravity vector is less than 1 degree.

During the deployment phase, the internal state machine oscillates between incrementally deploying the boom and releveling the leveling subsystem. This prevents the tower from suddenly becoming unstable and ensures a steady controlled tower deployment.

III.VIII Mock Lander

In order to make this phase of the MELLTT design as close to a flight-ready version as possible, a mock lunar lander was constructed to address three constraints described above: power, communications and leveling. The mock lander houses the main power system and the main computer and provides a platform to support MELLTT. In order to test the MELLTT leveler, the mock lander includes a movable platform that allows the entire system to be tilted. Fig. 8 shows the CAD of this mock lunar lander.

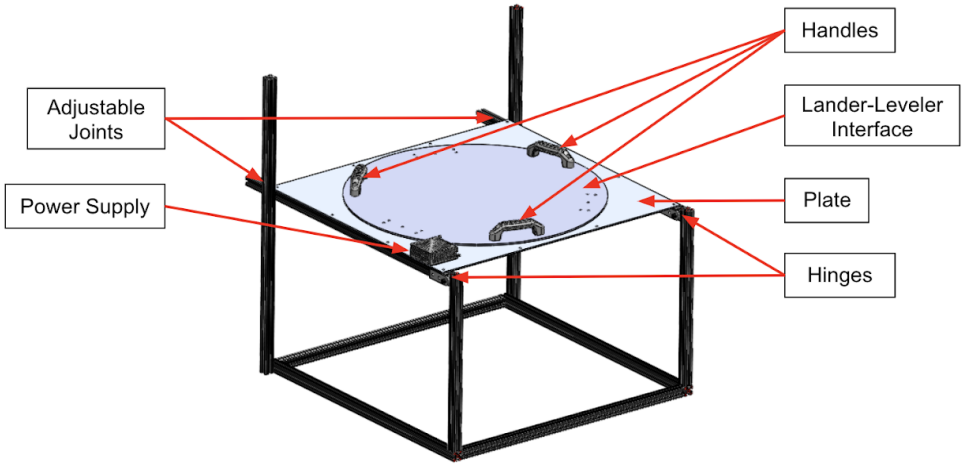

Figure 8: CAD of the MELLTT mock lunar lander with callouts identifying components.

III.IX Technical Specifications: Mass, Power, and Link Budgets

The power budget for the elevated platform of this demonstration system is 1.4W, which is the average production of the 1U CubeSat solar panels. The link budget for a 1W radio closes over 5km with 6dB margin. As currently designed and built, MELLTT has a total mass of ~21 kg, as shown in Table 3. In the remaining weeks of the challenge, the team will work to further reduce system mass.

In comparison to the original budget (shown in the fourth column of Table 3), the leveler subsystem went over slightly, the deployer subsystem went over significantly, the boom was under budget, and the upper bus was under budget significantly. The electronics were not included as a separate item in the original budget, but were in the final budget for ease of measurement since they were all connected. The final mass did not include a margin. The main cause of exceeding the original mass budget stemmed from a significant design change to the deployer subsystem. After detailed discussions with NASA Langley's Deployable Composite Boom team and independent testing conducted by the MIT team, the design was updated to include not just a "pushing" mechanism but also a "pulling mechanism." The puller added ~5 kg to the deployer subsystem mass. In addition to the puller mechanism, the MELLTT prototype includes some electronic components that would not be part of the flight payload, such as a ~0.8 kg power source. Without the pulling mechanism and the electronics not needed for flight, the total system mass would be 15.7 kg, just 5% over the original mass budget. From a systems perspective of the lunar lander's payload mass, MELLTT saves mass for other payloads, which would also justify exceeding the single-payload 15 kg mass budget. By using MELLTT for power beaming, communication relay or imaging, other payloads could reduce their mass by having smaller batteries, smaller antennas and radios, and smaller or no cameras. This mass saving can be rigorously documented using the NASA-standard Equivalent System Mass methodology [10] but such a calculation is beyond the scope of this report as we do not control the designs of the payloads that would gain a mass benefit from MELLTT. In this case, the overall lander payload mass constraint could likely be met even if MELLTT exceeded its individual payload mass constraint by ~5 kg because MELLTT would allow other payloads to decrease their masses.

Table 3: Mass of MELLTT prototype

Subsystem	Actual Mass (kg)	Proposal Budget (kg)	Comparison
Leveler	3.0	2	150.0%
Deployer	12.2	5	244.0%
Boom	0.10	1	9.7%
Upper bus	1.2	5	24.0%
Electronics	5.04	0	N/A
Margin	0	2	N/A
Total	**21.5**	**15.0**	

III.X Integration with External Systems

MELLTT interfaces with two sets of external systems. The elevated payload platform interfaces with client payloads, while the leveling subsystem interfaces with the lander.

The payload platform interfaces with client payloads through the top plate. The top plate includes nine mounting points for client payloads, arranged in a radially-symmetrical pattern. This symmetry ensures that the payload platform remains balanced atop the boom when client payloads are integrated, since client payloads can be added in opposite mounting slots in pairs. Each mounting slot contains a standardized interface and provides the ability to route cables connecting client payloads to the platform's power bus (with access to either 5 or 12 V) and communications with the lander (via the platform's integrated WiFi radio, compliant with the radio standard for CLPS landers [5]). Client payloads are provided with data and power through this interface, but must be thermally isolated from the payload platform.

The leveler interfaces with the lander at the upper surface of the lander. The legs of the leveler bolt to the top surface of the lander, and the leveler and deployer rely on the lander for power. The leveler/lander interface is assumed to be thermally isolating. Data is transferred between MELLTT and the lander over a WiFi radio link standard for a CLPS lander [5].

IV. PROOF-OF-CONCEPT TESTING ON EARTH

IV.I Testing Facilities

The MELLTT team's reserved workspace is a private room in MIT Building 37. This room was provided by MIT's Department of Aeronautics and Astronautics. The reserved workspace was used for the majority of testing, since other test facilities on campus were not available. Some component and subsystem testing took place in team members' homes across the globe, including in Massachusetts, New York, South Carolina, Washington and Australia.

The team also used various machine shops on campus for custom-designed parts (such as the leveler subsystem's trunnion mounts) and received in-kind support for 3D printing from Formlabs.

IV.II Risk and Mitigation Plan

The team identified 46 technical and programmatic risks (for the Earth proof of concept), assessed each of them, and developed individual mitigation strategies. A full list of the risks can be found in a prior publication [11]. Table 4 shows the project risk matrix, with likelihood and impact assigned prior to mitigation. Each risk is identified as a technical subsystem risk (L##: leveler; D##: deployer; B##: boom; P##: payload/upper bus) or a programmatic risk (PG##).

Table 4: Risk matrix for all technical and programmatic risks.

Likelihood	**5**		PG04, PG14		PG13	
	4		PG06, PG10	PG11, PG12, PG15		
	3		PG05, PG18	PG08, PG16, PG17	PG03	B03, PG07
	2		L05	L08, PG09	P02, D05, D06, B02	L07, D03, PG02
	1		PG01	L01, L02	D01, D07, D08, D09, D10	L03, L04, L06, P01, P03, D02, D04, B01, B04, PG02
		1	**2**	**3**	**4**	**5**
	Impact					

The analysis revealed four high-risk items: B03, PG07, and PG13. Each of these is detailed in Table 5 with the mitigation that was implemented to decrease or eliminate the risk.

Table 5: Key risks and their mitigations.

ID	Description	Mitigation
B03	During deployment, boom uncoils rather than extends, causing a failure. Uncoiling is a risk identified by the NASA Langley Deployable Composite Boom team, who loaned us the boom used in the project.	Developed a pulling system in addition to the deploying system.
PG07	Lack of software experience on the team.	Recruited two team members with significant robotics experience to run the software team.
PG13	Lack of access to tools and NASA testing facilities.	Received access to MIT in August, when campus reopened for our category of research.

IV.III Integration Plan

After all subsystems were independently assembled and tested, system integration and testing proceeded in three steps, starting with the mock lander at the base of the system and progressing upwards by subsystem, as shown in Fig. 9. After each step, a functional test was conducted. After the full system was integrated, additional tests verified the functionality of the integrated demonstration article.

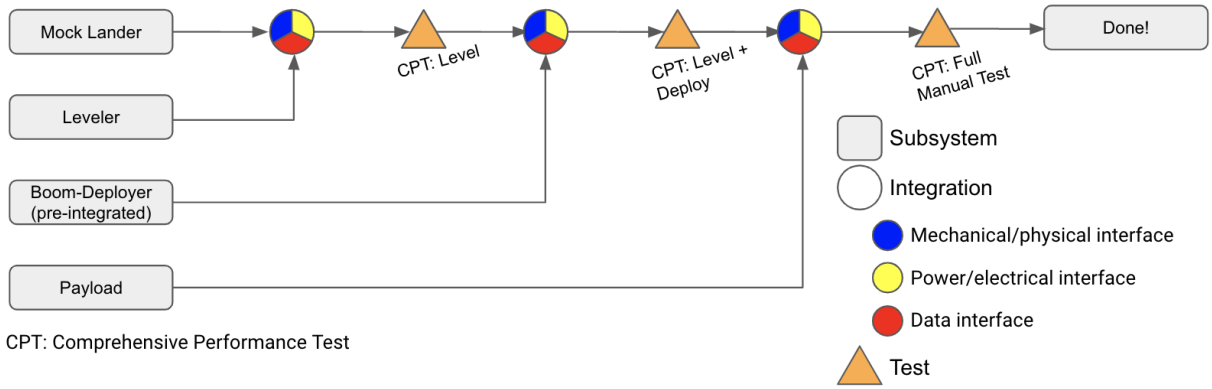

Figure 9: System integration plan, including a functional test after each integration.

IV.IV Testing Plan

For the Earth proof of concept design, the project team developed a test plan with four phases as shown in Fig. 10: 1) test in lab environment, 2) test in relevant environment, 3) test for launch and flight and 4) test for surface operations.

Phases 1 and 2 were planned as part of the BIG Idea project, with phases 3 and 4 left for future development to bring the payload to flight readiness. While phase 1 testing is complete, continued COVID-19 restrictions at NASA and MIT prevented the team from pursuing phase 2 tests. The phase 1 testing was broken out into detailed test plans for each subsystem, which included tasks for component and subsystem assembly, integration, and testing. These were tracked in an integration and testing Gantt chart throughout the duration of the build phase of the project. Following subsystem testing, the system was integrated (as discussed in Section IV.III) and system tests were performed after each integration. Upon completing the integration, a full system test was conducted to confirm functionality.

By completing phase 1 testing, MELLTT has achieved TRL 4, "analytical and experimental critical function and/or characteristic proof-of-concept" [12], through system testing in a laboratory environment. Of particular importance, the successful deployment of the composite boom in Earth gravity proved that the boom could be deployed in lunar gravity, which is ~⅙ Earth gravity.

The MIT team is pursuing additional funding to continue development, which would leverage phases 2-4 of the testing plan to continue increasing MELLTT's TRL until it is ready for launch. Two NASA funding opportunities are being pursued: 1) the team responded to NASA's PRISM [13] request for information (RFI) as a collaboration with NASA Langley and Germany's DLR, and 2) the team submitted a proposal to NASA's LuSTR solicitation [14] with two industry collaborators.

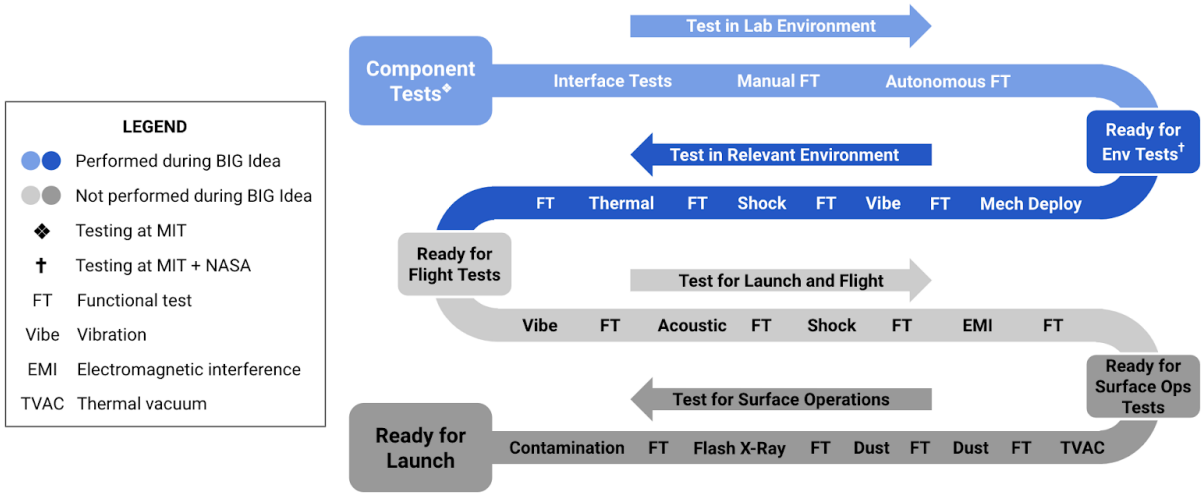

Figure 10: Initial test plan to progress from concept to ready for launch, highlighting the phases originally planned to be completed during the BIG Idea competition.

For the Earth proof-of-concept, the majority of limitations that stem from operating within a PSR (such as degraded communications, lack of light, abrasive regolith) were not incorporated in testing because MELLTT is not intended to operate within a PSR, but rather from outside of a PSR. For operating outside of a PSR, the team had to consider constraints such as the temperature environment near the lunar south pole and the possibility of landing on a slope. A thermal analysis is discussed in Section IV.VI and a mock lunar lander created for testing on slopes is discussed in Section III.VIII.

While the PSR operational constraints were not incorporated into MELLTT testing, they were considered in design to ensure that the system would be able to provide services to distal assets within a PSR. The main PSR constraints that MELLTT can help overcome are issues with power and communications. MELLTT's elevated payload platform includes a power generation system that, if scaled

up, can provide power beaming to distal assets both inside and outside of a PSR, and it also includes a communications system that can serve as a line-of-sight relay between the lander and distal assets.

IV.V Verification Plan

The verification plan for MELLTT involved mapping each requirement to a method of verification. The majority of requirements were verified through testing, with the remaining requirements verified through inspection or design review. Some requirements that were verified through testing were previously studied via analysis, such as static loading. The system verification mapping was maintained in two documents: the integration and testing Gantt chart (shown in Table 6) and the consolidated requirements spreadsheet (shown in Table 7).

Table 6: Snippet of integration and testing Gantt chart, showing mapping to requirements.

TASK TITLE	TASK ID	REQUIREMENTS TESTED
System Integration		
Integrate mock lander + leveler	SIT-01	L01
Test leveling on an incline	SIT-02	L02, L04, L05, L06, L07, L09, L10
Integrate boom/deployer to system	SIT-03	L12, D04, D06, D08
Test leveling + deploying on an incline	SIT-04	L02, L04, L05, L06, L07, L09, L10, D06
Integrate upper bus to system	SIT-05	B04, P03, P05, P11, P12, D06
Test full system (manual)	SIT-06	L02, L04, L05, L06, L07, L10, B01, B02, B03, B07, D06
Test full system (autonomous)	SIT-07	L09, D06

Table 7: Snippet of consolidated requirements spreadsheet, showing mapping to tests.

ID	Requirement	Explanation	Test(s)
L01	The leveler shall be capable of supporting 1.5x the weight of the deployer, boom and upper bus.	The leveling system and its motors must be able to handle leveling the deployer, boom, and payload deck. A 50% margin is included for a safety factor.	MLIT-05, LIT-19, LIT-20, LIT-21, SIT-01
L02	The leveler shall be capable of adjusting the roll and pitch of the system up to +/-12 degrees.	Slopes of up to 12 degrees are assumed to be possible post-landing, and the leveler must correct for these.	LIT-20, LIT-21, SIT-02, SIT-04, SIT-06
L03	The leveling system angular resolution, measured as deflection of the boom from the vertical, shall be 0.014 degrees (or finer).	The specified angular resolution limit results in instantaneous lateral displacement of ~5mm at a height of ~20m. This constraint mitigates excessive dynamic loads due to “jerking” of the platform if the leveling mechanism is used when the tower is fully deployed.	N/A - verified by design review

IV.VI Analytical Methods

As part of the PDR and CDR work to refine the design, the team conducted a preliminary system thermal analysis as well as various analyses on key aspects of subsystems.

Thermal Analysis

One of the primary path-to-flight questions considered was whether the existing design would be able to handle the temperature swings expected at the lunar south pole. Notably, at any given time, one side of the MELLTT system would be exposed to sunlight while the other side would face the coldness of space. A thermal analysis was conducted for the entire system to determine the temperature differentials expected from one side of the system to another, from which material requirements could be extrapolated to minimize thermal deformation stresses. An example of thermal analysis for parts of the MELLTT system is shown in Fig. 11, with the rest - including COMSOL thermal modeling - included in Appendix C for the sake of space.

The results of the thermal modeling informed material decisions, with the key finding that the existing material choices would be acceptable for the range of temperatures experienced on the moon. Additionally, the system would still function within specifications given the expected thermal deformations from warming and cooling of components.

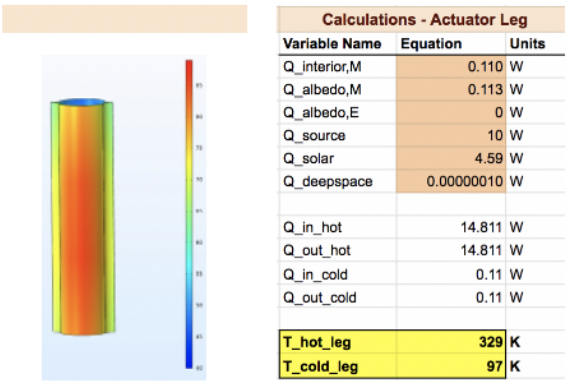

Calculations - Actuator Leg		
Variable Name	**Equation**	**Units**
Q_interior,M	0.110	W
Q_albedo,M	0.113	W
Q_albedo,E	0	W
Q_source	10	W
Q_solar	4.59	W
Q_deepspace	0.00000010	W
Q_in_hot	14.811	W
Q_out_hot	14.811	W
Q_in_cold	0.11	W
Q_out_cold	0.11	W
T_hot_leg	**329**	**K**
T_cold_leg	**97**	**K**

Figure 11: Thermal modeling calculations of the leveler subsystem.

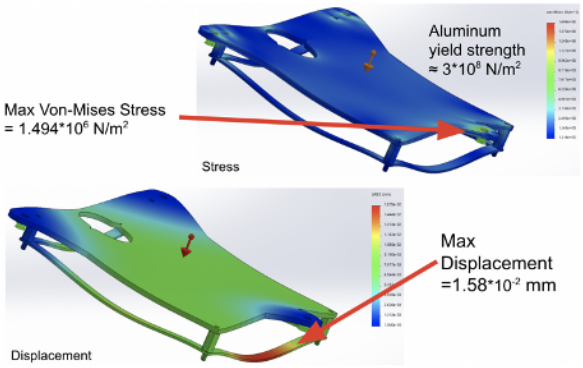

Fig. 12: Finite element analysis performed on leveler platform.

Structural Analysis

Before testing, finite element analysis was performed on the leveler platform in SolidWorks to ensure that it could handle the load of the system. As shown by the results in Fig. 12, the safety factor at the greatest stress concentrations was over 200. Due to the high safety factor, it was deemed acceptable to remove further mass from the plate for testing and to reduce the overall system mass.

Euler column buckling theory was used to calculate the approximate maximum buckling load for a cylindrical carbon fiber boom of similar material and thickness:

$$P_{cr} = \frac{AC\pi^2 E}{(l/k)^2} = 45 \text{ N}$$

Bending, compression, and torsional buckling failure loads were found to be higher, thus making buckling the primary failure mode. The expected weight supported by the tower for the prototype is 5.12 N, and the safety factor is 8.78.

IV.VII Experimental Methods

Leveling Subsystem

The functionality of the leveling system was experimentally tested by inclining the mock lander to a given angle, and then performing both a manual and automatic leveling sequence. Manual leveling sequences were performed first using the inbuilt Tolomatic linear actuator software and readouts from the accelerometer data, extending each leg sequentially to achieve a desired 0° pitch and roll angle relative to the gravity vector. Manual leveling allows for safer operation. Manual leveling was performed at 10° lander incline and confirmed the functionality of each linear actuator. Autonomous leveling utilized a

ROS control system, with the leveling system performing FK and IK with a feedback control loop to level the system to 0° pitch and roll angle relative to the gravity vector. Autonomous leveling was performed for 6° and 12° lander incline, on a level floor. Fig. 13 shows the accelerometer output from the 12° test. The initial cluster of spikes indicates the initial open-loop controller. The subsequent spikes in accelerometer data indicate activation of the feedback control loop, as the controller detects error in the initial leveled pose and attitude and actuates the legs accordingly. The figure shows the leveler successfully leveling the deployer plate to be aligned with the gravity vector (returning the x and y accelerometer components to 0 m/s^2). Multiple tests of the autonomous leveling system were conducted to verify this performance. In each case, successful leveling for 12° took between 40 and 90 seconds.

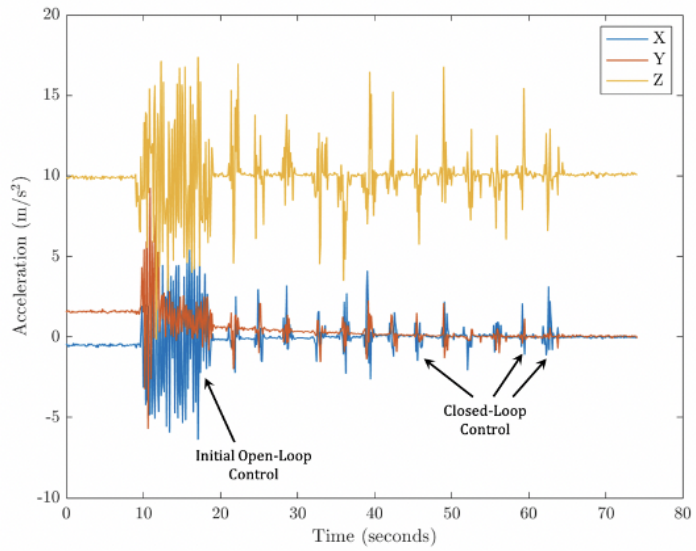

Figure 13: Leveler top plate accelerometer data during autonomous leveling for 12° incline. The X and Y accelerometer axis are aligned with the plane of the deployer mounting plate. The Z axis is normal to the deployer mounting plate.

Figure 14: Dynamic load test of the leveling subsystem

In order to verify the analytical load analysis, static and dynamic load tests of the leveling subsystem were conducted. The leveling subsystem was loaded with 11 kg, 22.5 kg and 34 kg of mass (a maximal load of 1.5 x total system mass to incorporate a 1.5 factor of safety) at lander angles of 0°, 6° and 12°. Static loads were conducted with the leveler stationary and inclined inline with the lander. Dynamic loads were conducted with the leveler beginning at an incline and leveling to 0° pitch and roll. Fig. 14 shows a photo taken during a dynamic load test. There was no measurable deformation of the leveler system in any of the static or dynamic load tests. In order to actuate the leveler with the 34 kg load at 12 degrees, the linear actuator motors used a peak torque of .45 Nm.

Deployment Mechanism Testing

Deployment integration and testing was performed in multiple steps. Throughout the process, care was taken to keep the boom safe from buckling or other disturbances that may cause permanent damage to the boom. The friction between the boom and the 3D-printed brace was tested before integration with the rest of the system. The distance traveled by the boom within the brace was measured using a TE Connectivity Measurement Specialties SP2-50 string potentiometer and the force required to push the boom was measured using a Vernier Dual-Range Force Sensor. The average friction was 1.908 N. Future work will investigate different materials, manufacturing methods, and lubricants to reduce the frictional force acting on the boom. Conversations with NASA Langley and MELLTT testing revealed the phenomenon of "blooming", which is when the boom unspools on the spool instead of outward due to frictional force on

the boom; to prevent this from occurring, the MELLTT team added a motorized pulling mechanism to overcome the frictional force of the 3D printed brace.

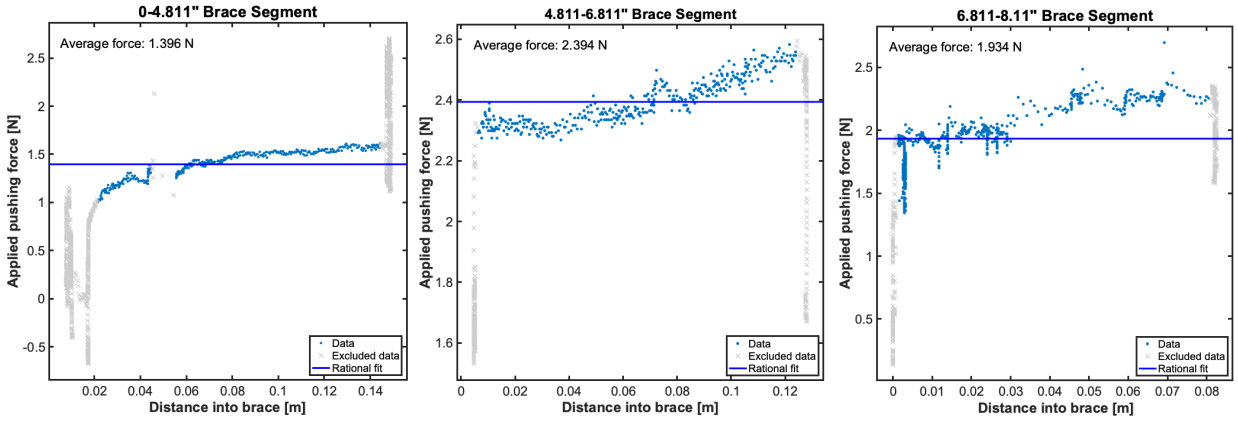

Figure 15: Results from friction testing between boom and 3D-printed brace.

As part of the pulling mechanism, rollers were manufactured and tested iteratively with an assorted set of form-fitting revolved geometries and a variety of sized rubber point-of-contact rollers. Since rollers of different sizes will have the same angular velocity (all being on the same shaft), their tangential velocity at the point of contact with the boom will not be equal. For this reason, some slipping is expected when using the rollers, and the frictional force that is displacing the boom, will be both kinetic and static. During testing, a stick-slip phenomenon was seen in all roller configurations. Ultimately, the best roller configuration for deployment and mitigating disadvantageous slipping was an 8-roller (4 on each side) configuration shown in Fig. 4a. The two outer larger rollers help to guide the boom in the right direction, and offer some pulling force, however the main pulling force comes from the two middle rollers, which are able to have better grip on the boom, because they are pressing on a stiff part of the boom.

The distance from the top of the 3D printed brace to the top of the tower when fully deployed was measured to be 1.52 meters. At this deployed height, the boom and deployer subsystem was tested for dynamic response to disturbances. The accelerometer located in the top platform was used to determine the natural frequencies of the system. In Fig. 16, a Fourier transform is performed on the accelerometer data in each direction; the natural frequency of the boom in the x-direction is 3.86 Hz, and approximately 2.95 Hz in the y-direction. In future work, the natural frequency will be characterized as a function of height, where it is expected that stiffness decreases with height. In addition, the damping ratio may be determined by measuring the displacement of the boom over time.

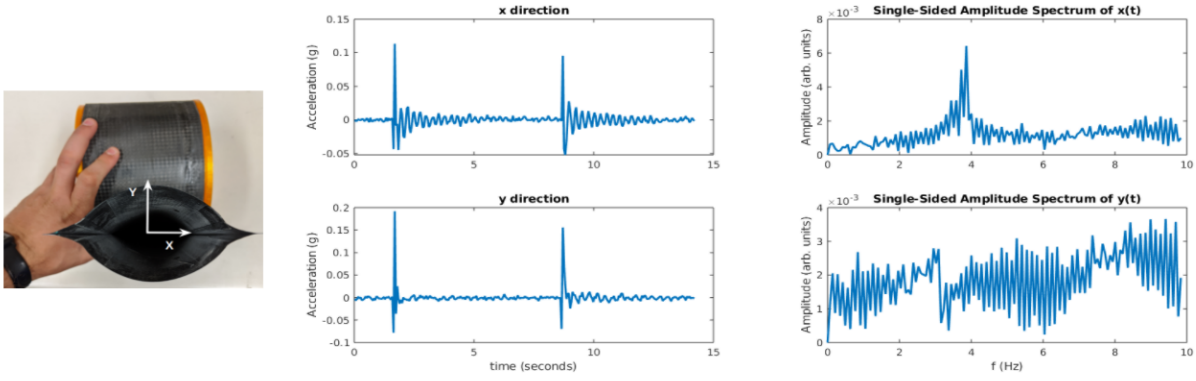

Figure 16. Acceleration data from the top of the fully deployed 2 meter boom (extending 1.52 meters above the 3D printed brace), after a series of disturbances to the base. A fourier transform reveals the natural frequencies of the boom in the x and y direction to be 3.86 Hz and 2.95 Hz, respectively.

Elevated Payload Platform Subsystem

The upper bus subsystem's main quantitative testing result is of the power load, which has not occurred yet. This testing will be completed prior to the final presentation in January.

IV.VIII Testing Results

The main outcome of MELLTT testing is a functional prototype of a deployable tower, including autonomous leveling, successful deployment and retraction of the tower, and 360° rotation and imaging from the upper bus. This functionality is shown in the demonstration video submitted with this report. In addition to this demonstration, quantitative testing was performed to characterize the performance of each subsystem. These tests were carried out with the 2 m lenticular boom and have validated the following design decisions, thereby advancing the MELLTT prototype to TRL 4:

- Three linear actuators for kinematic leveler: proof of concept performance and structural stability validated under both static and dynamic loads.
- Deployment mechanism: proof of concept validated for both deployment and retraction using combined unspooling and roller systems, with bracing.
- Pointing capability as a service with interface to the top of the deployable tower: proof of concept validated for corner case of fast pointing

In addition to validating the current MELLTT conceptualization, the testing performed has provided valuable information that will drive future design iterations. For example, the frictional test of the deployer's 3D printed PLA plastic brace will inform iterations in brace geometry and can be repeated as needed with new brace materials and different booms. Deployer motor torque specifications can now be determined with greater accuracy. The natural frequency of the deployed boom found during testing is an essential piece of knowledge for future development, so that other subsystems and payloads on the lunar lander can avoid operating at this frequency while the tower is deployed.

Testing has also revealed a number of challenges with the current MELLTT system. For instance, the leveler linear actuators tend to unscrew from the deployer plate. This can be mitigated by using left-hand threaded universal joints as well as adding thread-locking adhesive and wedge-locking washers to ensure a stable connection. Additionally, the deployment system encountered challenges with the roller puller system. A stick-slip phenomenon was observed as the outer rollers contact the boom at a higher tangential velocity than that of the smaller rollers. Ideally, the kinetic coefficient of friction of the outer rollers should match the static coefficient of the inner rollers. The roller system also encountered difficulty with retraction. In the prototype, the shaft-bearing tolerance was a loose slip-fit. The axial play in the roller shaft bearings causes the boom to become misaligned during retraction. Press-fit bearings with preload will likely solve this issue, however a one-directional sprag clutch will also be implemented, so the rollers can idle during retraction.

In addition to improving upon these difficulties, upgrades can be made to make the system more efficient. Many of these updates are included in the path to flight section, encompassing improvements in mass, power, structural stability, and boom friction.

A repeat of all functional tests with longer booms is planned for AY 2020-2021, namely with the 6 m commercial boom purchased by the team, and with the 16.5 m NASA boom when it becomes available.

IV.IX Challenges and Mitigations

The biggest challenge to testing was COVID-19. The pandemic prevented the MELLTT team from gaining access to NASA testing facilities and a majority of MIT testing facilities. COVID also resulted in the team being dispersed across the globe, from both U.S. coasts to Cyprus to Australia. The scope of testing had to be significantly reduced, and the remaining testing had to incorporate shipping time between team members. Rather than shipping from Australia to the U.S., the results of component and subsystem design and testing that was conducted in Australia was implemented into hardware by team members in the U.S. with instruction from the Australian students.

The second most significant challenge was identified when we received feedback from our NASA mentor, post-PDR, that the push mechanism for the deployer subsystem as originally designed (barrel,

flap, bracers) would likely lead to blooming of the deployed boom. In response, we designed and added a puller system using rollers positioned above the bracers. This had the added benefit of increasing the overall stability of the tower.

IV.X Safety Plan and Protocols Followed

An official standard operating procedure (SOP) was written for the team's on-campus laboratory space by a team member who was previously a safety officer for a hazardous chemical manufacturing plant. The SOP was reviewed and approved by MIT's EHS department, which included a walk-through of the space and written procedures. All team members were trained on the SOP prior to their use of laboratory facilities for prototyping activities. The SOP was modified in April to reflect the change in state caused by the COVID pandemic.

The team incorporated protocols from the safety plan into operations for assembly, integration and testing for students working from home and in the on-campus lab space. This included the purchase of safety glasses for every member of the team (to prevent COVID contamination caused by sharing), gloves for handling of the composite booms, and end caps for 80/20 to prevent cuts from the sharp edges, to name a few. Besides standard safety protocols, on-campus work also adhered to MIT's COVID-19 regulations, which included procedures such as regular testing of people working on campus, mask wearing, social distancing, and regular cleaning [15].

V. PATH TO FLIGHT

A framework for cataloging the steps in the operating sequence is used to investigate the design changes necessary to convert the Earth prototype being developed for BIG Idea into a flight article. In the majority of cases, the required path to flight change is substitution of hardware with a space-qualified part that accomplishes the same delivered function. This change will address thermal, vacuum, radiation, and dust concerns not experienced on Earth. In Table 8, underline indicates a required path to flight design change while *italics* indicate that the Earth prototype component or operation is largely ready for flight.

Table 8: Integrated Concept of Operations and Path to Flight Design Changes

Concept of Operations: Stage of Operation	**CONOPS Stage Enabled by Earth Prototype System**	**Path to Flight Design Changes to Support Flight System Operations**
Pre-launch integration with lander	Mechanical integration of Earth prototype packaging with a model of a CLPS lander deck	Design/materials to ensure adiabatic thermal interface between payload and lander deck
Survive through launch acoustic environment	Prototype packaging, which will differ necessarily from flight packaging	Integration and subsystem swaps; flight hardware acoustic tests
Survive space environment during transit and landing on the Moon (Fig. 2, Step 2 & 3)	Prototype avionics and initial thermal design appropriate for Earth prototype packaging, to contain costs	Incorporate flight-proven, radiation-hardened avionics and a space-qualified thermal design
Post-landing, pre-deployment test (Fig. 2, Step 4)	Semi-automated or manual testing and diagnostics	Incorporate flight-tested automation, telemetry and telecontrol
Open cover, carry out leveling operations (Fig. 2., Step 4)	Use flight-like leveling actuators to level deployer within Earth's gravitational field	*None - easier in reduced gravity environment,* verify thermal and dust performance

Lock the deployer in the level position (Fig. 2, Step 4)	Flight-like locking system capable of withstanding "leaning tower torques" at 1g; test at MIT facilities	*Non - flight system will operate easier in reduced gravity environment,* verify thermal and dust performance
Deploy tower to test height (2 m) (Fig. 2, Step 4)	Flight-like tower deployment system, deploying vertically to a height of 2 m under Earth gravity from simulated lander deck	*For boom, none/minor software change (easier in reduced gravity environment),* but replace deployer motor with a flight qualified model
Perform diagnostics while partially deployed for GO/NO GO full deployment decision	Wireless connection between top deck / deployer avionics; verify tower is vertical with respect to Earth gravitational field	*None/minor software change - easier in reduced gravity environment,* verify thermal and radiation performance
Contingency: tower departs from vertical while deploying	If departure from vertical detected, retract boom, re-level, re-deploy	*None/minor software change - easier in reduced gravity environment,* verify thermal and dust performance
Deploy tower to 16.5m height (Fig. 2, Step 5) (For deviations from nominal: see contingency)	Flight-like deployment system: slow deployment, monitoring top deck IMU for deviations from vertical	*None/minor software change - easier in reduced gravity environment,* verify thermal and dust performance
Validate repeater functionality by parroting back lander transmission (Fig. 2, Step 5)	Prototype repeater mounted on tower top deck will not be space-qualified	Design/procure and integrate actual flight payloads (repeater, imager)
Perform elevated deck rotation test, validate using imager data (Fig. 2, Step 5)	Slowly rotate top deck to deliver pointing / rotisserie service to payload	Replace with a flight-qualified actuator to provide top deck pointing
Contingency: tower departs from vertical while operating	If dynamic departure (swaying), cease operations until oscillation dampens. If static departure (bent mast), re-level and restart nominal operations.	Future designs of leveling base may incorporate active or passive damping systems to address boom vibration / shock.
Return all test data to Earth	Transmit data from payload to lander	Replace with flight payloads

Path to Flight Case Study: Long Range Radio Communication

To facilitate long distance communication to other assets inside and outside the PSR, MELLTT's payload deck is designed to support a 900 Mhz ISM Band transceiver. Using an omnidirectional antenna which allows for good coverage independent of pointing, such a 1 W transceiver, the system would provide 20 dB link margin, with 1 Mb/s over 2 km to assets inside of the crater. When accounting for diffraction effects on the PSR rim, and scattering effects on the crater itself, MELLTT can achieve over 80% crater coverage from a single tower. For large scale infrastructure development, the system can be expanded to a mesh network supporting multiple daisy-chained devices, including additional towers, and sensor systems in the PSR. With a higher power, 2 W transceiver, communications with an orbiter may also be achieved; the link budget summaries for these payload options are provided in Table 9.

Table 9: Long Range Radio Communication Link Analysis for 900 Mhz Transceiver.

	Tower to Crater Inside	**Tower to Tower**	**Tower to Satellite**
Range (kms)	2.0	21.4	400.0
Transmit power (W)	**1.0**	**1.0**	**2.0**
Bit rate (bps)	1,000,000	5,000,000	64,000

Link margin (dB)	20.1	7.75	3.26

Path to Flight Case Study: Real-Time Computing Subsystem

On the flight system, the mission-supporting computing systems would implement a real-time and deterministic execution structure. The design of the hardware would incorporate the functions of the modular components of the proof-of-concept system into a single printed circuit board (PCB). This singular PCB would handle all of the processing, sensing and communication, thus saving space and minimizing energy usage. Due to the cosmic radiation and thermal exposure, the on-board computer will periodically scrub the memory for bit-level memory errors and correct any discrepancies.

The operating system on the flight hardware would be a real-time operating system (RTOS) optimized for high reliability, timing determinism and low memory usage. The software onboard the system would implement a robust state machine capable of self-testing, error detection and contingency procedures. A watch-dog timer would be implemented to automatically reset the hardware in response to unforeseen faults. A basic diagram of the state machine is shown in Fig. 17 [16].

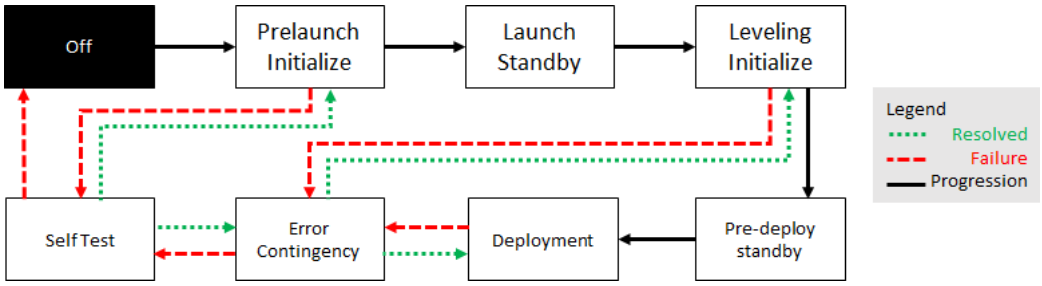

Figure 17: State Transition Diagram for On-board Computer System

Path to Flight Case Study: Guy Wires

To facilitate taller towers and greater mass payloads, guy wire support systems may be added; a system of guy wires has been evaluated in the TNX-Tower non-linear FEA package. With a 30 meter tower and a hypothetical 5 kg payload mass, a set of three mid-point anchored guy wires yields a 43% improvement in tilt performance under dead load compared to a system without the guy wires. With a significant disturbance such as a seismic load, these improvements are even more pronounced, as shown in Table 10.

Table 10: Analysis of guy wire performance in different configurations and loading patterns.

Guy Wire Configuration	Tilt Performance under Dead Load (degrees)	Tilt Performance under Mag. 5 Seismic Load (degrees)
Three at Top	2.3	12.1
None	2.1	7.0
Three at Top and Three Midway	1.4	2.5
Three at Midway Only	1.2	2.3

VI. TECHNICAL MANAGEMENT

VI.I Timeline

The COVID-19 pandemic had a significant impact on the schedule of the project because access to lab facilities was lost, team members were spread out across the globe, procurement of parts was often delayed, and because of the general unexpected tumult introduced into team members' lives.

Table 11: Timeline of key activities for the MIT BIG Idea team

Month	Key Activities
02/2020	● BIG Idea awards announced; received first stipend ● Visited composite boom vendors
03/2020	● MIT lab safety plan submitted and approved ● COVID-19 pandemic began affecting project; lost access to campus
04/2020	● Conduct PDR with MIT, NASA and industry advisers
05/2020	● Submitted BIG Idea mid-term report ● Received NASA Langley DCB 2 m boom
06/2020	● Received second stipend ● Conducted CDR with MIT, NASA and industry advisers ● Placed orders, began component and subsystem assembly and testing
07/2020	● Worked on component and subsystem assembly and testing
08/2020	● Worked on component and subsystem assembly and testing ● Regained access to campus
09/2020	● Worked on component and subsystem assembly and testing ● Began preparation for system integration and testing
10/2020	● Began system integration and testing ● Finalized deployer subsystem design to accommodate NASA boom geometry ● Received CTD 2 m and 6 m booms; began designing deployer subsystem to accommodate CTD boom geometry
11/2020	● Finished all testing needed for proof-of-concept demonstration ● Submitted technical paper and proof-of-concept demonstration files
12/2020	● Close out system testing ● Make final refinements to design
01/2021	● Final presentation at 2020 BIG Idea Virtual Forum

VI.II Budget

The original approved budget as submitted immediately following the award in February 2020 was revised at the time of payment of the Phase II funds as shown in Table 12 to account for post-PDR changes to design, for COVID-19 impacts to our project plan and for the additional sponsorship of $8,873.11 received by MASGC. Actual expenses to date as at the time of writing of this report were at or below these revised budgets for each item with the exception of boom and deployer where the 9% budget overrun of $4,541 was more than covered by the $9,403 allocated prototype margin. The budget revisions vs. the original approved budget were driven by the following COVID-19 events that impacted the project:

- The 16.5 m deployable composite boom that would have been borrowed from NASA Langley DCB became unavailable, so at the time of writing this report, the prototype has been built and tested using only the sample 2 m NASA boom.
- Traveling to the ASCEND conference and to NASA sites for testing could not take place, so the budgeted traveling funds were not spent and were classified as unallocated margin.
- NASA testing centers were not available, so the originally budgeted testing funds were reallocated to purchase a 6 m commercial boom instead.

An authorization for a no-cost extension to January 2021 has been received by NIA and a final account of actual expenses broken down by phase will be made available to NIA and to the two funding sponsors

at that time as we are currently continuing work on integrating our deployer with the 6 m boom, with expenses for the changes to our prototype being covered from both accounts.

Table 12: MELLTT financial budget

	Phase I Budget	Phase II Budget	Actual Expenses Paid (both phases) in $ and as % of budget		Comments
PROTOTYPE PARTS					
Leveler	$ 10,000		$ 8,257	83%	*Completely redesigned leveler following feedback to proposal*
Deployer and Boom	$ 6,236	$ 43,500	$ 54,277	109%	*Langley 16.5m loaner boom not available due to COVID-19*
Cubesat Payload Platform	$ 6,680	$ -	$ 3,296	49%	*Used cheaper motor instead of flight-proven motor*
Integration & Testing materials	$ 2,000	$ 3,000	$ 2,364	47%	*Testing was descoped (COVID)*
Tools, Tooling, Software Dev kits	$ 9,850	$ 3,000	$ 5,650	44%	*Testing was descoped (COVID)*
Prototype margin	$ 4,453	$ 4,950	$ -		*Margin allocated to deployer following design changes*
SUBTOTAL PROTOTYPE	**$ 39,219**	**$ 54,450**	**$ 73,844**		
TESTING COSTS					
Mechanical deployment test fees	$ -	$ -	$ -		*NASA closed due to pandemic*
TVAC test fees	$ -	$ -	$ -		*NASA closed due to pandemic*
Vibration test fees	$ -	$ -	$ -		*NASA closed due to pandemic*
Testing margin		$ -	$ -		*NASA closed due to pandemic*
SUBTOTAL TESTING	**$ -**	**$ -**	**$ -**		
TRAVEL AND ADMIN					
Airfares, hotels, cars, food	$ 3,813	$ 19,709	$ 1,813	8%	*ASCEND trip cancelled due to pandemic*
Forum / ASCEND registrations		$ 6,375	$ 375	6%	*Virtual event, no registration fee*
MIT Overhead and time costs	$ 25,517	$ 8,873	$ 34,390	100%	
Travel and Admin margin	$ 1,467	$ 3,496	$ -		
SUBTOTAL TRAVEL AND ADMIN	**$ 30,797**	**$ 38,453**	**$ 36,578**		
UNALLOCATED MARGIN / FUNDS NOT YET SPENT	$ 5,153	$ 4,702	$ 62,352		*Project continues in 2021 to convert deployer for 6m boom*
GRAND TOTAL	**$ 75,169**	**$ 97,605**	**$ 172,774**		*Phase 2 total increased by $8,873.17 following decision of MASGC to cover MIT's overhead*

VI.III Covid-19 Impacts and Adaptation

As mentioned throughout the report, the COVID-19 pandemic had a significant impact on the MELLTT project. Below is a summary of the main impacts and the adaptations developed to address them.

Table 13: COVID-19 impacts and adaptations

COVID-19 Impact	Adaptation
Lost access to MIT lab March-July	Conducted a significant amount of component and subsystem testing in team members' homes
Unable to pursue testing at NASA facilities	Descoped test plan and increased resources for functional testing
Unable to conduct environmental testing (e.g. vibration) at MIT	Descoped test plan

Team spread across three countries and several time zones	Relied heavily on Zoom and Slack for communications. Shipped hardware between team members.
NASA unable to send 16.5 m boom	Procured 2 m boom from NASA as well as a 2 m and 6 m boom from CTD; team is continuing to work on integrating the 6 m boom with our deployer and payload

VII. CONCLUSION AND NEXT STEPS

As robots and humans travel to the lunar south pole and begin to explore its permanently shadowed regions, they will face many key challenges that threaten their missions. Among these will be a lack of line-of-sight communications from a sunlit ground station to assets inside the PSR. The Multifunctional, Expandable Lunar Lightweight, Tall Tower (MELLTT) project described here is a novel solution to this problem, enabling important science and exploration missions that may otherwise prove infeasible, too risky or too complex without this proposed tower infrastructure.

Alternative proposed tower designs are heavy (estimated to require between 100 and 1000 kg) and sized to carry large payloads (~100 kg) to relatively small heights (~10 m). For exploratory missions, these heavy tower systems have been cost-prohibitive due to a launch cost of $1.2M/kg [17]. MELLTT's design of a lightweight (~20 kg) and tall tower (~16.5 m) with a small payload is a valuable and low-cost option (~$74,000 for prototype) that can assist missions by providing power and signal relays, as well as line-of-sight for payload instruments. The low mass of the structure enables more than an order of magnitude of cost savings, while the taller height enables the tower to have greater line-of-sight range to peer over crater rims into PSRs. Both of these design aspects are critical in enabling affordable exploration, as lower cost and greater capabilities will enable future lunar missions.

REFERENCES

1. Johanson RT, Jang D, Kononov E, Luu M, Morgan SJ, Todd J, et al. What could we do with a 20 meter tower on the Lunar South Pole? Applications of the Multifunctional Expandable Lunar Lite & Tall Tower (MELLTT). ASCEND 2020. American Institute of Aeronautics and Astronautics; 2020. doi:10.2514/6.2020-4108

2. Fernandez JM, Rose G, Stohlman OR, Younger CJ, Dean GD, Warren JE, et al. An Advanced Composites-Based Solar Sail System for Interplanetary Small Satellite Missions. 2018 AIAA Spacecraft Structures Conference. American Institute of Aeronautics and Astronautics; 2018. doi:10.2514/6.2018-1437

3. Reveles J, Lawton M, Fraux V, Gurusamy V, Parry V. In-Orbit Performance of AstroTube: AlSat Nano's Low Mass Deployable Composite Boom Payload. Small Satellite Conference. 2017. Available: https://digitalcommons.usu.edu/smallsat/2017/all2017/76/

4. National Institute of Aerospace. 2020 Lunar PSR Challenge Details. In: NASA's Breakthrough Innovative and Game-changing (BIG) Idea Challenge [Internet]. 2020 [cited 27 Sep 2020]. Available: https://bigidea.nianet.org/competition-basics/

5. Astrobotic. Peregrine Lunar Lander Payload User's Guide Version 3.2. In: NASA's Breakthrough Innovative and Game-changing (BIG) Idea Challenge [Internet]. Jun 2019 [cited 27 Sep 2020]. Available: http://bigidea.nianet.org/competition-basics/

6. Duennebier F, Sutton GH. Thermal moonquakes. J Geophys Res. 1974;79: 4351–4363. doi:10.1029/JB079i029p04351

7. Nakamura Y, Latham GV, Dorman HJ. Shallow moonquakes-depth, distribution and implications as to the present state of the lunar interior. Lunar and Planetary. 1979. Available: http://adsabs.harvard.edu/full/1979LPSC...10.2299N

8. Furqan M, Suhaib M, Ahmad N. Studies on Stewart platform manipulator: A review. J Mech Sci Technol. 2017;31: 4459–4470. doi:10.1007/s12206-017-0846-1

9. Faessler M, Mueggler E, Schwabe K, Scaramuzza D. A monocular pose estimation system based on infrared LEDs. 2014 IEEE International Conference on Robotics and Automation (ICRA). 2014. pp. 907–913. doi:10.1109/ICRA.2014.6906962

10. Levri JA, Vaccari DA, Drysdale AE. Theory and application of the equivalent system mass metric. SAE Technical Paper; 2000. Available: https://www.sae.org/publications/technical-papers/content/2000-01-2395/

11. Lordos GC, Amy C, Browder B, Chan M, Dawson C, do Vale Pereira P, et al. Autonomously Deployable Tower Infrastructure for Exploration and Communication in Lunar Permanently Shadowed Regions. ASCEND 2020. American Institute of Aeronautics and Astronautics; 2020. doi:10.2514/6.2020-4109

12. National Aeronautics and Space Administration. NASA Technology Readiness Levels. In: National Aeronautics and Space Administration [Internet]. [cited 27 Sep 2020]. Available: https://www.nasa.gov/sites/default/files/trl.png

13. E.11 Payloads and Research Investigations on the Surface of the Moon NSPIRES Solicitations

Summary. In: National Aeronautics and Space Administration [Internet]. 14 Feb 2020 [cited 29 Nov 2020]. Available: https://nspires.nasaprs.com/external/solicitations/summary.do?solId=%7B03464E24-4AFA-781E-200C-956EE283CD8A%7D&path=&method=init

14. Lunar Surface Technology Research (LuSTR) Opportunities NSPIRES Solicitations Summary. In: National Aeronautics and Space Administration [Internet]. 15 Jul 2020 [cited 28 Nov 2020]. Available: https://nspires.nasaprs.com/external/solicitations/summary.do?solId=%7B0BA38320-8F63-2EAF-D97B-0AB42AF17C35

15. MIT Covid-19 Info Center. In: MIT [Internet]. 2020 [cited 28 Nov 2020]. Available: https://covid19.mit.edu/

16. Wertz JR, Everett DF, Puschell JJ. Space mission engineering: the new SMAD. Microcosm Press; 2011.

17. Lunar Delivery. [cited 29 Nov 2020]. Available: https://www.astrobotic.com/lunar-delivery

APPENDIX A: LEVELER INVERSE KINEMATICS CALCULATIONS

The control objective for the leveler is to orient the platform supporting the boom deployer in such a way that a vector normal to the surface of the platform is aligned with the lunar gravity vector. Given the 3-axis components of the gravitational acceleration as measured by an accelerometer mounted on the top of the lunar lander, the leveler controller must determine the desired leg lengths which will bring the platform in alignment with gravity. Note however that the leveler system has 3 degrees of freedom (pitch, roll and vertical translation) whereas only 2 degrees of freedom (or 2 legs) would only be needed in theory to level the platform. The height is therefore an arbitrary value and can be set by the user to its minimum possible value in order to lower as much as possible the center of mass of the system.

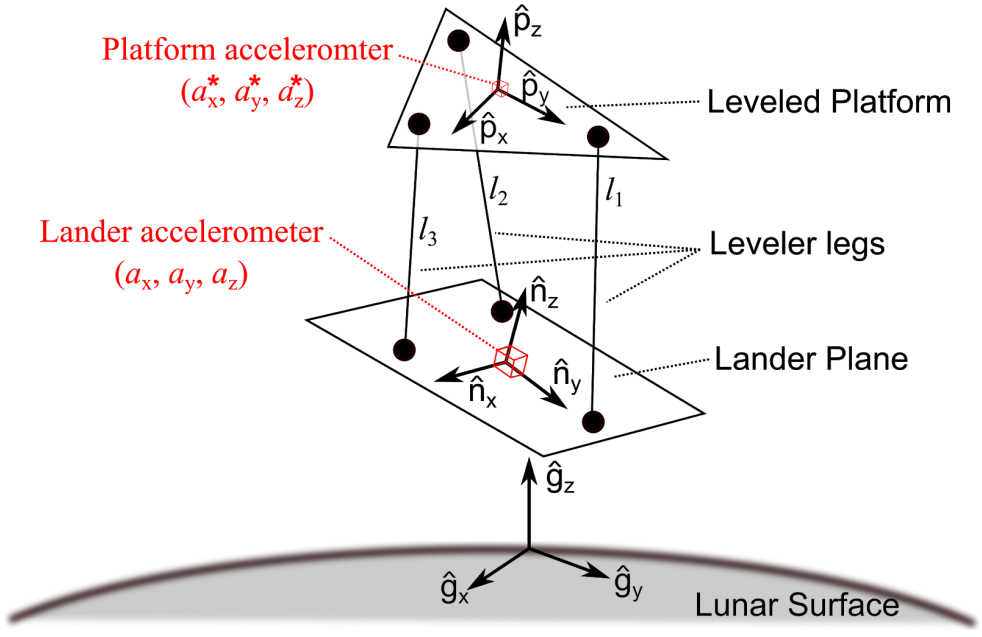

Measurements from the accelerometer mounted on the lander base (a_x, a_y, a_z) are used to determine the current orientation of the lander relative to the gravitational field. Let θ_n and δ_n be the pitch and roll angles of the lander's reference frame in the global reference frame. They can be calculated as

$$\theta_n = \text{asin}\left(\frac{a_x}{\sqrt{(a_x)^2+(a_y)^2+(a_z)^2}}\right) \tag{1}$$

$$\delta_n = \text{asin}\left(-\frac{a_y}{\sqrt{(a_x)^2+(a_y)^2+(a_z)^2}}\, cos^{-1}(\theta_n)\right) \tag{2}$$

There are five unknowns in the inverse kinematics problem which describe the desired orientation of the leveled platform in the lander reference frame: x_0, y_0, γ_p, θ_p and δ_p. These are respectively the x and y components of the leveler\s origin in the lander base reference frame and the yaw, pitch and roll Euler angles describing the rotations necessary to go from the lander base reference frame to the platform reference frame. Let $\mathbf{p}_x$ and $\mathbf{p}_y$ be the unit vectors of the platform`s reference frame in plane with the platform and $\mathbf{g}_z$ be the gravity vector. Then the platform is considered levelled if the two following equations are respected:

$$\mathbf{p}_x \cdot \mathbf{g}_z = 0 \tag{3}$$

$$\mathbf{p}_y \cdot \mathbf{g}_z = 0 \tag{4}$$

Expanding these equations results in

$$\begin{gathered}\sin(\theta_n)\cos(\theta_p)\cos(\gamma_p) + \sin(\theta_n)\cos(\theta_n)\cos(\delta_n) \\ - \sin(\delta_n)\sin(\gamma_p)\cos(\theta_n)\cos(\theta_p) = 0\end{gathered} \tag{5}$$

$$\begin{gathered}- \sin(\delta_n)\cos(\theta_n)\cos(\theta_p)\cos(\delta_n) \\ - \sin(\theta_n)(\sin(\gamma_n)\cos(\delta_n) - \sin(\theta_n)\sin(\delta_n)\cos(\gamma_n)) \\ - \sin(\delta_n)\cos(\theta_n) (\cos(\delta_p)\cos(\gamma_p) + \sin(\theta_p)\sin(\delta_p)\sin(\gamma_p)) = 0\end{gathered} \tag{6}$$

Moreover, since each leg of the platform has a hinge pivot at the bottom, this means that the top attachment point of each leg can be viewed as constrained to a virtual plane fixed in the base reference frame. These describe three constraints which can be written as

$$\begin{gathered}y_0 + (0.5773503)L_p\sin(\gamma_n)\cos(\theta_n) \\ - H_p(\sin(\delta_p)\cos(\gamma_p) - \sin(\theta_p)\sin(\gamma_p)\cos(\delta_p)) = 0\end{gathered} \tag{7}$$

$$\begin{gathered}(0.5)y_0 + (0.8660254)x_0 \\ + (0.25)L_n(\cos(\delta_n)\cos(\gamma_n) + \sin(\theta_n)\sin(\delta_n)\sin(\gamma_n)) \\ + (0.8660254)H_p(\sin(\delta_p)\sin(\gamma_n) + \sin(\theta_n)\cos(\delta_p)\cos(\gamma_p)) \\ - (0.25)L_n\cos(\theta_n)\cos(\gamma_n) - (0.1443376)L_p\sin(\gamma_n)\cos(\theta_p) \\ - (0.5)H_n(\sin(\delta_n)\cos(\gamma_n) - \sin(\theta_n)\sin(\gamma_n)\cos(\delta_n)) \\ - (0.4330127)L_p(\sin(\gamma_p)\cos(\delta_p) - \sin(\theta_p)\sin(\delta_p)\cos(\gamma_p)) = 0\end{gathered} \tag{8}$$

$$(0.8660254)x_0 + (0.1443376)L_p\sin(\gamma_p)\cos(\theta_p)$$

$$+ (0.25)\mathrm{Lp}(\cos(\delta_n)\cos(\gamma_n) + \sin(\theta_n)\sin(\delta_n)\sin(\gamma_n) + (0.8660254)H_n(\sin(\delta_n)\sin(\gamma_n) + \sin(\theta_p)\cos(\delta_p)\cos(\gamma_p)) + (0.4330127)L_p(\sin(\gamma_n)\cos(\delta_n)-\sin(\theta_n)\sin(\delta_n)\cos(\gamma_n)) + 0.5H_p(\sin(\delta_p)\cos(\gamma_p) - \sin(\theta_p)\sin(\gamma_p)\cos(\delta_p)) - 0.5y_0 - 0.25L_p\cos(\theta_p)\cos(\gamma_p) = 0 \quad (9)$$

Finally, from equations (5), (6), (7), (8) and (9), one can solve for the 5 unknowns (x_0, y_0, γ_n, θ_n and δ_n). Finding an algebraic solution to this system of nonlinear equations is however nontrivial: instead, a numerical approximation is used. Recovering the desired leg lengths (l_{1d}, l_{2d} and l_{3d}) once the position and orientation of the top platform is known can easily be computed using this solution and the following three equations derived using the geometry of the problem:

$$(l_1)^2 + (2/3)L_n\cos(\theta_n)\cos(\gamma_p)(L_n-1.732051x_0) + 2H_n\cos(\theta_n)\cos(\delta_n)(H_n-z_0) + 2H_n y_0(\sin(\delta_n)\cos(\gamma_n) - \sin(\theta_p)\sin(\gamma_p)\cos(\delta_p)) + (1.154701)H_n(L_n-(1.732051)x_0)(\sin(\delta_n)\sin(\gamma_n) + \sin(\theta_n)\cos(\delta_n)\cos(\gamma_p)) - (H_n)^2 - 1/3(L_n)^2 - (y_0)^2 - (H_n - z_0)^2 - (1/3)(L_n-1.732051\,x_0)^2 - (1.154701)L_p y_0\sin(\gamma_p)\cos(\theta_p) - 1.154701)L_p\sin(\theta_p)(H_n-z_0) = 0 \quad (10)$$

$$(l_2)^2 + (0.5773503)L_n\sin(\theta_p)(H_n-z_0) + L_n\sin(\delta_n)\cos(\theta_n)(H_n-z_0) + (0.1666667)L_n\cos(\theta_n)\cos(\gamma_n)(L_n+ (3.464102)x_0) + 2H_n\cos(\theta_n)\cos(\delta_n)(H_n-z_0) + 0.5L_n(L_n-2y_0)(\cos(\delta_n)*\cos(\gamma_n) + \sin(\theta_p)\sin(\delta_n)\sin(\gamma_n)) + (0.2886751)L_n(L_n+(3.464102)x_0)(\sin(\gamma_n)\cos(\delta_n) - \sin(\theta_n)\sin(\delta_n)\cos(\gamma_n)) - (H_n)^2 - 1/3(L_n)^2 - (H_n-z_0)^2 - 1/4(L_n-2y_0)^2 - 0.08333333(L_n+(3.464102)x_0)^2 - (0.2886751)L_n\sin(\gamma_n)\cos(\theta_p)(L_n-2y_0) - (0.5773503)H_n(L_n+(3.464102)x_0)(\sin(\delta_n)\sin(\gamma_n) + \sin(\theta_p)\cos(\gamma_n)\cos(\gamma_p)) - H_p(L_n-2y_0)(\sin(\delta_p)*\cos(\gamma_p)-\sin(\theta_p)\sin(\gamma_p)\cos(\delta_p)) = 0 \quad (11)$$

$$(l_3)^2 + (0.5773503)L_p\sin(\theta_n)(H_n-z_0) + (0.1666667)L_n\cos(\theta_n)\cos(\gamma_n)(L_n+(3.464102)x_0) + (0.2886751)L_n\sin(\gamma_n)\cos(\theta_n)(L_n+2y_0) + 2H_p\cos(\theta_p)\cos(\delta_p)(H_n-z_0) + (0.5)\mathrm{Lp}(L_n+2y_0)(\cos(\delta_n)\cos(\gamma_n)+\sin(\theta_n)\sin(\delta_n)\sin(\gamma_n)) + H_n(L_n+2y_0)(\sin(\delta_n)\cos(\gamma_n) - \sin(\theta_n)\sin(\gamma_n)\cos(\delta_n)) - (H_n)^2 - (1/3)(L_n)^2 - (H_n-z_0)^2 - (0.25)(L_n+2y_0)^2 - 0.08333333(L_n+(3.464102)x_0)^2 - L_n\sin(\delta_n)\cos(\theta_p)(H_n-z_0) - 0.5773503(H_n)(L_n+ (3.464102)x_0)(\sin(\delta_n)\sin(\gamma_n) + \sin(\theta_n)\cos(\delta_n)\cos(\gamma_n)) - (0.2886751)L_p(L_n+ (3.464102)x_0)(\sin(\gamma_p)\cos(\delta_p) - \sin(\theta_p)\sin(\delta_p)\cos(\gamma_p)) = 0 \quad (12)$$

where the definition of all the known parameters are included in Table A-1.

Table A-1: Constants Describing the Geometry of the Leveler Platform

Constants	Definition
L_p	Distance between leg top attachment points on platform (assumed same between all adj. attachment points)
L_n	Distance between leg bottom attachment points on base (assumed same between all adj. attachment points)
H_p	Vertical offset between each of the leg top attachment points and the origin of the platform reference frame
H_n	Vertical offset between each of the leg bottom attachment points and the origin of the base reference frame

APPENDIX B: UPPER BUS SUBSYSTEM POWER AND MASS CALCULATIONS

Table B-1: Payload subsystem normal and lower power mode estimates, with negative power indicating battery charging.

	Power Draw (W)	
Component	**Normal**	**Low Power**
1x Raspberry Pi Camera HQ	1.375	0.4
1x Arduino	0.294	0.294
1x Raspberry Pi Zero W	1.1	0.7
4x Solar Panels	-2.74	-2.74
Net Power	0.029	-1.346
w/ 5% Safety Factor	0.03045	-1.1393

Table B-2: Payload Subsystem mass budget

Component	Component Mass	Quantity	Total Mass (kg)	Source
Frame Structure	0.4	1	0.4	Solidworks mass of 0.4 kg (including all frame components + electronic plate but without nuts and bolts).
Payload-Boom Interface				
Motor	0.06	1	0.06	https://www.pololu.com/product/3400/specs
Solar Panels	0.02	4	0.08	https://www.digikey.com/product-detail/en/ixys/SM531K12L/SM531K12L-ND/9990471
Battery	0.155	1	0.155	https://www.adafruit.com/product/353
Software	0.2	1	0.2	Boards, camera, lens
Miscellaneous	0.04	25	1	Nuts + bolts, solar panel connectors, small parts.
20% Margin	0.385	1	0.379	
Total			**2.27**	
Measured Total			**1.2**	Prototype Assembly

APPENDIX C: THERMAL MODELING CALCULATIONS

C.I Leveler Subsystem

Table C-1: Thermal modeling calculations of the leveler subsystem

Calculations - Actuator Leg		
Variable Name	**Equation**	**Units**
Q_interior,M	0.110	W
Q_albedo,M	0.113	W
Q_albedo,E	0	W
Q_source	10	W
Q_solar	4.59	W
Q_deepspace	0.00000010	W
Q_in_hot	14.811	W
Q_out_hot	14.811	W
Q_in_cold	0.11	W
Q_out_cold	0.11	W
T_hot_leg	**329**	**K**
T_cold_leg	**97**	**K**

Calculations - Leveler Platform		
Q_interior,M	3.202	W
Q_albedo,M	0.564	W
Q_albedo,E	0	W
Q_source	0	W
Q_solar	53.56	W
Q_deepspace	0.00000011	W
Q_in_hot	57.33	W
Q_out_hot	57.33	W
Q_in_cold	3.20	W
Q_out_cold	3.20	W
T_hot_platform	**250**	**K**
T_cold_platform	**121**	**K**

C.II Deployer Subsystem

Thermal modeling of a simplified deployment subsystem was done using COMSOL.

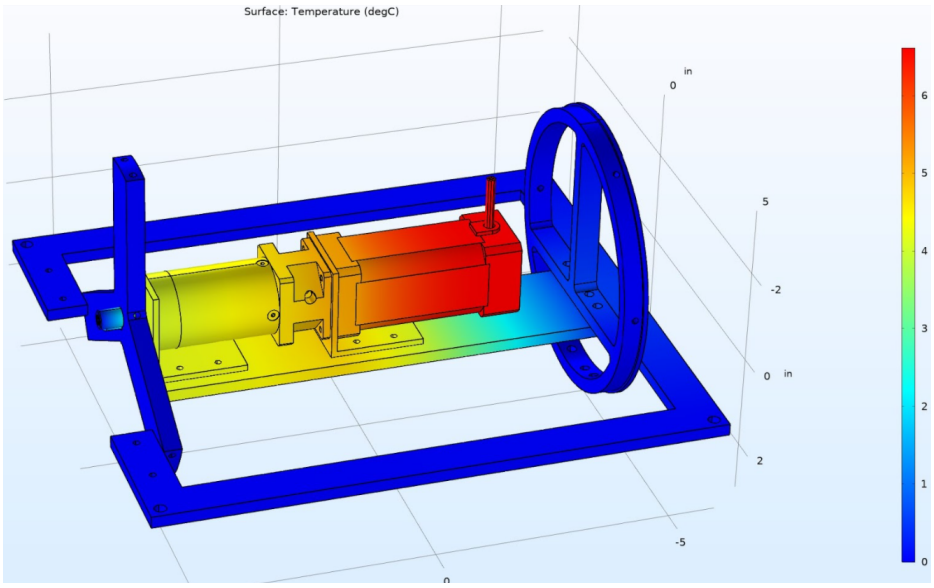

Figure C-1. COMSOL thermal modeling of a simplified deployer.

Due to the heat generated by the motor (~10 W), to overcome friction, the flight motor should operate at a more efficient speed. This can be done with a higher gear ratio or a worm gear, which would allow the motor and gearbox to be smaller and lighter.

C.III Boom Subsystem

Thermal modeling of the boom was done using COMSOL using it's unique lenticular geometry derived from a SolidWorks model.

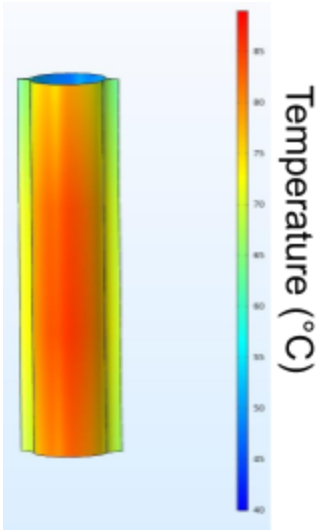

Figure C-2: COMSOL thermal modeling of the boom

Using COMSOL, conduction, radiation, solar flux, and lunar flux was applied to the 3D lenticular boom. This resulted in the Sun side of the boom 50°C hotter than the dark side, and resulted in a deflection of 15 mm for a 16.5 m boom.

C.IV Elevated Payload Platform Subsystem

A similar thermal analysis was performed for the elevated payload platform. Using standard space-grade hardware, the elevated payload platform has an operational temperature range of between 273 K and 318 K, with do-not-exceed limits of 253 K to 318 K (allowing for reduced heating requirements during transit). A bulk thermal analysis suggests that the upper payload platform will reach a maximum temperature of 302 K during nominal operation if 5 mil aluminized Kapton is used for albedo modification on the upper surface of the platform, and a minimum temperature of 168 K without additional mitigation. To avoid exceeding the minimum temperature requirement, the flight design will need to include heating elements, but the size of those heating elements will depend on the thermal load imposed by client payloads. In the absence of additional payloads, the platform would require internal heaters delivering 9 W (for transit and night survival) and 12.5 W (for operation).

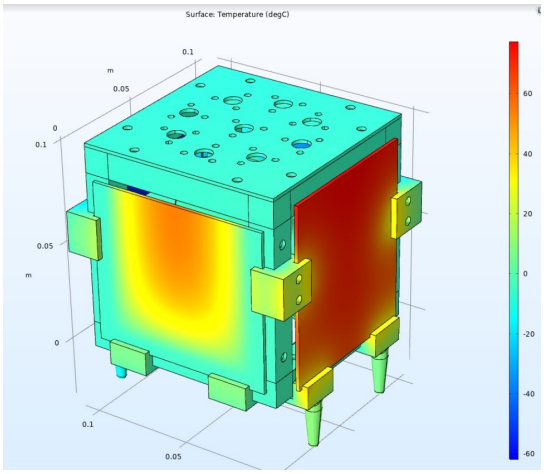

Figure C-3. COMSOL thermal modeling of the upper platform.

ACKNOWLEDGMENTS

The authors would like to thank the National Institute of Aerospace, NASA's Space Technology Mission Directorate and the Massachusetts Space Grant for funding support; the NASA Langley Deployable Composite Booms Team and FormLabs for in-kind support and MIT's Department of Aeronautics and Astronautics for access to facilities and services. Mentorship, advice and/or feedback from BIG Idea Judges, NASA Langley, NASA Kennedy Space Center, Jet Propulsion Laboratory and Robots5, LLC was invaluable to the development of our design.